PHILOSOPHICAL TRANSACTIONS OF THE ROYAL SOCIETY A MATHEMATICAL, PHYSICAL & ENGINEERING SCIENCES

On the Structure of Tilt Grain Boundaries in Cubic Metals I. Symmetrical Tilt Boundaries

A. P. Sutton and V. Vitek

Phil. Trans. R. Soc. Lond. A 1983 **309**, 1-36
doi: 10.1098/rsta.1983.0020

Phil. Trans. R. Soc. Lond. A **309**, 1–36 (1983) [1]
Printed in Great Britain

ON THE STRUCTURE OF TILT GRAIN BOUNDARIES IN CUBIC METALS I. SYMMETRICAL TILT BOUNDARIES

By A. P. Sutton† and V. Vitek
Department of Materials Science and Engineering, and the Laboratory for Research on the Structure of Matter, University of Pennsylvania, Philadelphia, Pennsylvania 19104, *U.S.A.*

(*Communicated by J. W. Christian, F.R.S. – Received* 1 *April* 1982)

CONTENTS

An atomistic study of tilt grain boundary structures in f.c.c. metals has been made. The principal aim of this study is to understand the structure of long-period ('general') tilt boundaries. Boundaries for which $\Sigma \leqslant 491$ were considered, where Σ is the reciprocal density of coincidence sites. The work is presented in three parts. In this paper three series of atomistic studies of symmetrical tilt boundaries in aluminium and copper are reported. One of the main objectives is to determine whether the stress fields of localized grain boundary dislocations exist in boundaries deviated far from any short-period boundary orientations. On the basis of the results of these studies, a new structural classification of grain boundaries is introduced. Certain boundaries are found to be the fundamental structural elements of other boundaries nearby in the misorientation range. Boundaries that consist of contiguous sequences of one type of fundamental structural elements are called favoured; all other boundaries are called non-favoured. It is found that favoured boundaries are not always associated with the lowest possible values of Σ and that the same boundaries are not necessarily favoured in all metals with the same crystal structure. With use of the pair interactions to calculate the atomic level stress tensor, the hydrostatic stress fields of the boundaries are displayed. In all cases

† Present address: Department of Metallurgy and Science of Materials, University of Oxford, Parks Road, Oxford OX1 3PH, U.K.

considered the stress fields of distinct, localized intrinsic grain boundary dislocations were found in non-favoured boundaries. The concept of continuity of boundary structure with misorientation is introduced. It is shown that continuity of boundary structure requires unique boundary structures at all misorientations. With use of this concept it is demonstrated how one can predict the atomic structure and stress field of any non-favoured boundary between two known, successive favoured boundaries. It is also found that an isolated discontinuous change in boundary structure between two successive favoured boundaries may exist, depending on their translation states. Some earlier atomistic studies of tilt boundaries in f.c.c. and b.c.c. metals are reinterpreted in the light of this work.

1. Introduction

In the past, grain boundaries have been classified as 'special' or 'general'. The difference between special and general boundaries has never been defined clearly from a structural viewpoint. Instead, special boundaries acquired their distinction because of their exceptional properties (for a review see Pumphrey 1976). For example, special boundaries frequently have relatively low energy (for a review see Goodhew 1980) and they also appear to have higher mobilities than general boundaries, at least when impurities are present in solution (Aust & Rutter 1959). It was always found that special boundaries were associated with coincidence site lattices (c.s.ls) possessing a low reciprocal density, Σ, of coincidence sites (see for example Kronberg & Wilson 1949). Furthermore, the planes of these boundaries are parallel to low-index planes of the corresponding c.s.l., and therefore the structures of special boundaries are two-dimensionally periodic with relatively small repeat cells. The converse has also been inferred many times in the literature, i.e. a boundary with a relatively small repeat cell is special. Thus, boundaries associated with a relatively high planar coincidence site density, Γ, are identified as special (see for example Brandon *et al.* 1964). However, Goodhew (1980) has pointed out that in faceting experiments facets associated with the highest available values of Γ are observed only occasionally.

A central problem in studies of the structure of high-angle grain boundaries that has attracted much theoretical and experimental work is the determination of their dislocation structure. The Frank–Bilby equation (Frank 1950, Bilby 1955) relates the net Burgers vector, $\boldsymbol{B}$, of interfacial dislocations crossing any vector $\boldsymbol{p}$ in the interface and the lattice deformations $\boldsymbol{S}_1$ and $\boldsymbol{S}_2$ converting the reference lattice into real lattices 1 and 2 respectively:

$$\boldsymbol{B} = (\boldsymbol{S}_2^{-1} - \boldsymbol{S}_1^{-1})\,\boldsymbol{p}. \tag{1}$$

In this equation $\boldsymbol{B}$ is defined in the reference lattice. Christian & Crocker (1980) have pointed out that $\boldsymbol{B}$ is not defined uniquely by equation (1) because $\boldsymbol{S}_1$ and $\boldsymbol{S}_2$ may be replaced by $\boldsymbol{U}_1\boldsymbol{S}_1$ and $\boldsymbol{U}_2\boldsymbol{S}_2$ where $\boldsymbol{U}_1$ and $\boldsymbol{U}_2$ are homogeneous lattice-invariant deformations represented by unimodular matrices with integral elements. Lattice symmetry operations form a subset of $\boldsymbol{U}$, but more generally $\boldsymbol{U}_1$ and $\boldsymbol{U}_2$ have the effect of shearing the two crystal lattices 'into themselves' resulting in no change in either them or the interface. However, $\boldsymbol{B}$ is affected by alternative choices of $\boldsymbol{S}_1$ and $\boldsymbol{S}_2$ and there is an infinite number of such descriptions for a given interface and reference lattice. Henceforth, this multiplicity will be referred to as the multiplicity of the first kind. For example, the plane of any symmetrical tilt boundary may be described as the invariant plane of a simple shear in the crystal lattice (Christian 1975). In O-lattice† terms the O-point

† If both real lattices are allowed to interpenetrate throughout all space, the O-lattice is defined by Bollmann (1970) as the set of points that have the same internal unit cell coordinates with respect to lattices 1 and 2.

lattice then becomes an O-plane lattice with exact lattice fit in the boundary plane (Bollmann 1970). For this description $\boldsymbol{B} = 0$ so that any symmetrical tilt boundary may be described as dislocation free. But if one regards the symmetrical tilt boundary as being obtained by pure rotations $\pm \frac{1}{2}\theta$ about the axis $\boldsymbol{t}$ in the crystal lattice, to give a total misorientation of θ, one obtains $\boldsymbol{B} = 2 \sin(\frac{1}{2}\theta)\boldsymbol{p} \wedge \boldsymbol{t}$. The first description can assume a physical significance when, for example, the boundary migrates by a shear mechanism as in deformation twinning. The second is the familiar representation by equal and opposite rotations of the median lattice about the tilt axis.

A second kind of multiplicity in the dislocation description of an interface is the choice of reference structure for defining $\boldsymbol{S}_1$ and $\boldsymbol{S}_2$. The atomic structure of the interface is independent of the choice of reference structure and in this respect the choice of reference structure is arbitrary. However, $\boldsymbol{B}$ is dependent on this choice and, furthermore, Bollmann (1970) has demonstrated that $\boldsymbol{B}$ is 'quantized' into discrete grain boundary dislocations (g.b.ds) whose Burgers vectors are also dependent on the choice of reference structure. The most commonly used reference structures for grain boundaries in cubic materials are the ideal lattice and 'special' boundaries. The Burgers vectors of g.b.ds based on the ideal lattice are those of lattice dislocations, as in Read & Shockley (1950). As the misorientation increases the separation of lattice dislocations becomes so small that they become indistinguishable and it is then considered more physically meaningful to use a 'special' boundary as a reference structure. The Burgers vectors of g.b.ds based on a special boundary reference structure are vectors of the d.s.c. lattice† associated with the c.s.l. to which the special boundary belongs (Bollmann 1970). The total dislocation content of a high-angle boundary is then divided into the primary (lattice) dislocations comprising the special boundary reference structure and the secondary (d.s.c.) dislocations accommodating the angular deviation from this reference structure. Alternatively, the special boundary reference structure may sometimes be regarded as the invariant plane of a simple shear and therefore dislocation free. A principal goal of many geometrical analyses of grain boundary structure has been the determination of a choice of reference structure that provides the most physically realistic description of the g.b.d. structure of a given boundary. Bollmann (1970) claims that such a reference structure does indeed exist and is given by the condition that the unit cell of the corresponding O-lattice is maximized. As pointed out by Christian & Crocker (1980) this condition requires further restrictions for symmetrical tilt boundaries to eliminate unrealistic shear descriptions for high-Σ boundaries, which lead to dislocation-free descriptions of the boundary structure.

The infinite number of dislocation descriptions, due to the multiplicity of the first kind, apply to a given boundary and reference structure. All of these descriptions apply regardless of the atomic structure of the boundary and hence there does not exist a preferred choice of $\boldsymbol{S}_1$ and $\boldsymbol{S}_2$ as far as the atomic structure is concerned. However, certain properties of the boundary such as its migration by a shear mechanism or a diffusion mechanism may be more readily explained by invoking particular descriptions of the lattice deformation. The multiplicity of dislocation descriptions of the second kind applies to a given boundary and prescription for $\boldsymbol{S}_1$ and $\boldsymbol{S}_2$, and it stems from the infinite choice of possible reference structures. As described in §3, for a given atomic structure and interatomic potential it is possible to calculate the stress field of the boundary at the atomic level. Using this stress field one can select the most physically appropriate reference structure for the boundary in question. The most appropriate reference structure is that which exists between the g.b.d. stress fields. Thus all the dislocation character of the stress field of the boundary is accounted for.

† The d.s.c. lattice may be defined as the set of difference vectors between lattice vectors of real lattices 1 and 2.

PHILOSOPHICAL TRANSACTIONS OF THE ROYAL SOCIETY A MATHEMATICAL, PHYSICAL & ENGINEERING SCIENCES

In recent years, Gleiter and co-workers have claimed that the secondary g.b.d. description of high-angle grain boundary structure is of limited physical significance because the cores of these dislocations are delocalized at misorientations beyond a few degrees from special boundaries (Gleiter 1977*a*, *b*; Pumphrey *et al.* 1977). While it has been demonstrated that the theoretical arguments supporting this claim are fallacious (Vitek *et al.* 1979; Sutton & Vitek 1980*a*), the transmission electron microscope observations remain controversial (see for example Pumphrey & Goodhew 1979; Pond & Smith 1977). Until now little was known about the structure of high-Σ grain boundaries, partly because most atomistic studies have considered only 'special' boundaries (for a review see Vitek *et al.* 1980*a*). In this paper we present the results of three series of atomistic calculations of the structures of symmetrical tilt boundaries in aluminium and copper. In each series of calculations we have systematically varied the misorientation and included some high-Σ ($\Sigma \leqslant 491$) boundaries. We are thus able to follow the change in boundary structure with misorientation from one 'special' boundary to the next. The most significant result is that certain special boundaries, which we call favoured boundaries, are found to be the fundamental structural elements, called units, of longer-period tilt boundaries, which we call non-favoured boundaries. We have used the term favoured rather than special because some low-Σ boundaries are found to be non-favoured, while normally they would be classified as special. It is emphasized that this classification of boundaries is purely according to their structure and not their energy. A favoured boundary is composed of a contiguous sequence of units of only one type and those units are then defined to be in their ideal (undistorted) state. A non-favoured boundary in the misorientation range between two successive favoured boundaries is composed of well defined mixtures of two different units, of which at least one is the unit of one of these favoured boundaries. The favoured boundary units composing a non-favoured boundary are inevitably distorted. However, the relaxation is always such as to minimize these distortions and we believe it is this that gives favoured boundaries their structural significance. The local misorientation across a non-favoured boundary varies because each unit relaxes towards its ideal misorientation. The significant local misorientation difference between different adjacent units produces an incompatibility between them, which is the source of a g.b.d. stress field. Since the corresponding g.b.d. accommodates a local misorientation difference it may be regarded as a secondary g.b.d. The most physically appropriate choice of reference structure is then the favoured boundary represented by the majority units because such incompatibilities do not exist in this boundary. A favoured boundary is therefore free of secondary g.b.ds and may be regarded as free of all dislocations if it can be described as the invariant plane of a simple shear. Alternatively, a favoured boundary may be described as an array of uniformly and closely spaced primary, lattice dislocations accommodating the rotation from the ideal lattice. Thus although a favoured symmetrical tilt boundary may be described as dislocation free it is not locally stress free, as will be apparent in the stress fields shown below. Following Hirth & Balluffi (1973) we call these secondary dislocations intrinsic g.b.ds because they are an inseparable part of the equilibrium structure of the boundary and therefore they do not produce long-range stress fields. They are in contrast to extrinsic g.b.ds, which originate from lattice dislocations entering the boundary or from Bardeen–Herring sources in the boundary. This distinction is based on the premise that grain boundaries are free of long range stresses at equilibrium, which cannot be maintained always.

The structural unit model of Bishop & Chalmers (1968, 1971) is similar to the description of grain boundary structure presented here. This structural unit model is based on the crystallo-

graphic inevitability that a long-period boundary can always consist of strained units of shorter-period boundaries. It is never known *a priori* which boundary units to choose, what their atomic structures are and whether the same units compose boundaries nearby in the misorientation range. In this work it is found that the answers to these questions are dependent on the interatomic potential.

Throughout this study attention is focused on the following questions.

1. Are there any geometrical criteria for predicting which boundaries are favoured? Are the same boundaries favoured in all metals with the same crystal structure? Do favoured boundaries always have exceptional properties such as low energy?

2. What is the atomic structure of a non-favoured boundary with a misorientation that is far from that of any favoured boundary? To what extent can the structure be regarded as 'arbitrary' or 'disordered'? Do the intrinsic g.b.ds, based on the appropriate favoured boundary reference structure, retain any physical significance at such large deviations?

3. Consider two adjacent favoured boundaries, i.e. two favoured boundaries sharing the same rotation axis and such that no other favoured boundary exists in the misorientation range between them. How is the transition accomplished in the intervening misorientation range in terms of (i) the two sets of d.s.c. dislocations with their different Burgers vectors and spacings, and (ii) the atomic coordination? For example, the favoured boundaries may contain different compact polyhedra (Vitek *et al.* 1980*a*).

4. Which boundary properties can be used to determine favoured boundaries?

The work is presented in three parts. In this part I symmetrical tilt boundaries are studied and it is assumed that all boundaries considered are stable with respect to faceting. The following part II is concerned with the structure of asymmetrical tilt boundaries. A classification of tilt boundaries in cubic crystals is developed in part II that is based entirely on geometrical criteria; it indicates which tilt boundaries may be related by either intrinsic secondary g.b.d. arrays or faceting. The conclusions reached in parts I and II are further generalized in the following part III by introducing a new concept, which we call the decomposition lattice. The decomposition lattice indicates 'selection rules' for favoured boundaries that, under certain conditions, enable one to predict favoured boundaries. The results of several previous atomistic studies of relatively long-period tilt boundaries in f.c.c. and b.c.c. metals are reinterpreted and they are all shown to conform to the scheme propounded here. The applicability of the scheme to (001) twist boundary structures, calculated by Bristowe & Crocker (1978), has also been demonstrated (Sutton 1982). The extension of this development to mixed tilt and twist boundaries is discussed and an explanation of the physical basis of 'plane-matching dislocations' is offered in part III.

The three series of calculations of symmetrical tilt boundaries reported in this paper are as follows:

(i) $[1\bar{1}0]$ tilt axis in aluminium, $0 \leqslant \theta \leqslant 50.48°$,

(ii) [001] tilt axis in copper, $0 \leqslant \theta \leqslant 36.87°$,

(iii) $[11\bar{1}]$ tilt axis in aluminium, $0 \leqslant \theta \leqslant 60°$,

where θ is the angle of misorientation about the tilt axis. [001] Tilt boundaries in aluminium were studied by Smith *et al.* (1977) and some of the results of this paper are discussed in §7. Some relevant results of the study of [001] and $[1\bar{1}0]$ tilt boundaries in b.c.c. metals by Vitek *et al.* (1980*b*) are also discussed in §7. Preliminary reports of some aspects of this work have appeared in Sutton & Vitek (1980*b*), Sutton & Vitek (1981) and Sutton *et al.* (1981). All of the calculated structures referred to in this work are also given by Sutton (1981).

2. Method of calculation and interatomic potentials

The method of calculating the structure of tilt grain boundaries is essentially the same as that described by Pond & Vitek (1977), and more recently by Vitek *et al.* (1980*a*). A 'block', consisting of the atomic coordinates of an unrelaxed f.c.c. bicrystal containing a selected coincidence boundary, is first constructed in the computer. An equilibrium relaxed structure is found by minimizing the total internal energy with respect to all atomic positions subject to the constraint that the total volume of the block is constant. Relative displacements of whole layers parallel to the boundary are permitted as well as individual atomic relaxation. Thus an overall relative translation of the two grains parallel to the boundary may occur during the relaxation. A central force pair interaction is assumed between atoms. The total energy of the system is given by the sum of all pair interactions and a term that depends only on the *average* volume per atom in the block. Atomistic calculations of defect structures have used one of two possible constraints on the block: constant total volume or zero net hydrostatic pressure. Vitek *et al.* (1980*a*) have shown that identical energies are obtained with these two methods provided the linear approximation to the volume-dependent energy is assumed and a sufficiently large block is used. The only difference in the calculated structures is the presence of a long-range, elastic, compressive strain in the block obtained at constant total volume; the atomic configurations are otherwise identical. In addition, within the linear approximation to the volume-dependent energy the total energy is independent of any expansion of the block. It is therefore necessary to use a nonlinear approximation to the volume-dependent energy to define the expansion at a boundary uniquely.

Owing to the high-index nature of the boundary planes considered in this work, it was desirable to introduce a scheme of selective relaxation. This scheme is similar to the 'indicator method', devised originally for calculations of the core structures of dislocations (see for example Vitek & Yamaguchi 1981). The selective relaxation scheme used in this work was found to increase the speed of relaxation by as much as a factor of 30. A detailed description of the method has been given by Sutton (1981).

Two pair potentials have been used in this work. The potential for aluminium, constructed by Dagens *et al.* (1975) in the framework of pseudopotential theory, has been used extensively in previous studies of grain boundary structure (see references in Vitek *et al.* 1980*a*). Pond & Vitek (1977) found excellent agreement between translation vectors of several tilt boundaries in the $\Sigma = 3$ coincidence system calculated with this aluminium potential and experimentally determined values in aluminium obtained by an electron diffraction technique. In view of this, and the very good agreement with phonon dispersion curves (Dagens *et al.* 1975), and reasonable values of the stacking fault energy (Vitek 1975) it is felt that this potential accurately describes atomic interactions in aluminium (see also Taylor 1981, Jacucci & Taylor 1981, Jacucci *et al.* 1981). The potential shows long-range oscillations and it is therefore necessary to employ a cut-off radius, r_c, during atomistic relaxations. Pond & Vitek (1977), studied the effect of different choices of r_c and concluded that the atomic configuration of a boundary changed by less than 5 % when $r_c \geqslant 1.6a$, where a is the lattice parameter, but the calculated energies converged much more slowly. In this work we follow Pond & Vitek (1977) and use $r_c = 1.6a$, but we do not present boundary energies calculated with this potential. An empirical pair potential for copper, constructed by Crocker *et al.* (1980), has also been used in this work. This potential has been used in studies of twist boundaries by Bristowe & Crocker (1978) and Ingle & Crocker (1980), and symmetrical tilt boundaries by Crocker & Faridi (1980). The

validity of the pair potential approximation in copper is not as easily justified as it is in aluminium. Furthermore, the vacancy formation energy was used in the construction of this potential, and Jacucci *et al.* (1981) have shown that this is an incorrect procedure in metals with a high electron density. We therefore regard this potential as a model potential, rather than a potential that accurately represents atomic interactions in copper.

There are several significant differences between the forms of the potentials for aluminium and copper. The potential for copper terminates at third nearest neighbour separation in the ideal crystal ($r_c = 1.225a$), and rises more steeply than the potential for aluminium in the repulsive side. Whereas the potential for copper is negative at first nearest neighbour separation, the potential for aluminium is positive. It is hoped that by using such substantially different potentials the general conclusions of this study will be applicable to boundary structures in a broader range of metals. Owing to the absence of long-range oscillations in the potential for copper, the boundary energies could be calculated reliably, although, again, we do not expect to obtain agreement with experimental measurements of boundary energies in copper.

3. Methods of interpreting the results

A conventional method of presenting the calculated structure of a tilt boundary is to plot the atomic positions in projection along the tilt axis (see for example Smith *et al.* 1977). Atoms on different atomic planes along one period of the tilt axis are distinguished by different symbols (e.g. triangles, crosses, squares). If a rigid body translation of one grain with respect to the other parallel to the tilt axis exists then twice as many symbols are required. Of central importance in this work is the physical significance of the secondary dislocation description of a non-favoured boundary, based on the appropriate favoured boundary reference structure. The above plots may be used qualitatively to identify edge dislocations by looking for terminations of lattice planes parallel to the favoured boundary, but a more objective method has been used based on the hydrostatic stress field of the boundary. In an inhomogeneously deformed lattice the stress tensor $\sigma^l_{\alpha\beta}$ at ion l can be defined by the relation

$$\sigma^l_{\alpha\beta} = \frac{1}{2V^l}\sum_{l'}\frac{1}{|\boldsymbol{r}^{ll'}|}\frac{\mathrm{d}\phi(|\boldsymbol{r}^{ll'}|)}{\mathrm{d}|\boldsymbol{r}^{ll'}|}r^{ll'}_{\alpha}r^{ll'}_{\beta}, \tag{2}$$

where $\boldsymbol{r}^{ll'}$ is the relative position of ions l and l', $\phi(r)$ is the central force pair potential and V^l is the local atomic volume at the ion l. The summation is taken over all interacting ions, and all quantities are evaluated in the deformed lattice. This expression may be derived by considering the change in energy per unit volume, δE, when an infinitesimal homogeneous strain, $\delta\epsilon_{\alpha\beta}$, is applied to the inhomogeneously deformed lattice. To first order, δE is given by

$$\delta E = \delta\epsilon_{\alpha\beta}\sum_{l}\sigma^l_{\alpha\beta}. \tag{3}$$

It is important to note that $\sigma^l_{\alpha\beta}$ is defined without reference to any idealized state. The local stress tensor, equation (2), has been used extensively in atomistic studies of dislocation core structures (see for example Basinski *et al.* 1971, Duesbery *et al.* 1973) and recently in the identification and classification of structural defects in amorphous solids (Egami *et al.* 1980). The hydrostatic stress p^l is given by

$$p^l = \tfrac{1}{3}\sum_{\alpha}\sigma^l_{\alpha\alpha} = \frac{1}{6V^l}\sum_{l'}|\boldsymbol{r}^{ll'}|\frac{\mathrm{d}\phi(|\boldsymbol{r}^{ll'}|)}{\mathrm{d}|\boldsymbol{r}^{ll'}|}. \tag{4}$$

Thus, when the hydrostatic stress is evaluated in the ideal lattice, one obtains the negative of the Cauchy pressure. In a hydrostatic stress field map the hydrostatic stress at each atomic site is represented by an arrow, centred on that site, with length proportional to the magnitude of the local hydrostatic stress, the direction of which indicates its sign. Arrows pointing to the right indicate hydrostatic compression whereas arrows pointing to the left indicate hydrostatic tension. Because our interest lies in the perturbation caused by the boundary the Cauchy pressure is added to each p^l and this reduced hydrostatic stress is represented in the maps. The maximum hydrostatic stresses in these maps are of the order of the theoretical shear strength. The arrow length magnification varies from one map to another for normalization reasons, and therefore quantitative comparisons of different stress field maps cannot be made. An edge dislocation in the ideal lattice can be readily identified by its characteristic hydrostatic stress field, which consists of an alternation from compression to tension above and below its slip plane respectively. But the interpretation of the hydrostatic stress field of a symmetrical tilt boundary is not unique owing to the multiplicity of dislocation descriptions. In this work the dislocation description of a non-favoured boundary is always in terms of secondary dislocations accommodating the misorientation from the appropriate favoured boundary, as discussed in § 1. The total stress field of a non-favoured boundary is therefore interpreted as the superposition of the fields of these secondary dislocations and the field of the appropriate favoured boundary.

The definition of the local atomic volume, V^l, is not unique. In this work we have taken $V^l = (\frac{4}{3}\pi)\,(r^*)^3$ where r^* is half the smallest interatomic separation from the set of $|\boldsymbol{r}^{ll'}|$. A more satisfactory definition is to consider a weighted average of all members of the set of $|\boldsymbol{r}^{ll'}|$, as shown by Sutton (1981) and Sutton & Vitek (1982). The definition of V^l used here tends to exaggerate compressive stresses but the fields calculated with the two different definitions of V^l are qualitatively very similar.

An overall compressive stress exists in the relaxed blocks of atoms in this work. This is because the relaxations have been carried out at constant total volume. Hence, hydrostatic compression predominates over hydrostatic tension in the stress field maps. However, this is irrelevant to identifying cores of edge dislocations. They occur at the regions where there is a sharp transition from maximum hydrostatic compression to relative tension. By 'relative tension' we mean a large decrease in compression that may or may not actually be tension.

4. [1$\bar{1}$0] Symmetrical tilt boundaries in aluminium

4.1. *Introduction*

Three of the boundary structures studied here were calculated before: $\Sigma = 11\,(113)_1$ and $\Sigma = 9\,(114)_1$ structures may be found in Pond *et al.* (1979) and $\Sigma = 27\,(115)_1$ structure in Pond *et al.* (1978). The $\Sigma = 11$ boundary structure is composed entirely of capped trigonal prisms, whereas tetrahedra are the only compact polyhedra in the $\Sigma = 27$ boundary structure. A systematic series of calculations of boundaries in the range $31.59 \leqslant \theta \leqslant 50.48°$ was carried out to reveal how the change in atomic coordination occurs and to investigate the stress fields of the intervening boundaries. The results of this study are reported in § 4.2 and an analysis follows in § 4.3. Section 4.4 contains the results and analysis of the study of the range $0 \leqslant \theta \leqslant 31.59°$.

4.2. *Results for the range* $31.59 \leqslant \theta \leqslant 50.48°$

The boundaries selected in this misorientation range are listed in table 1. The boundary planes with respect to the upper and lower grains are shown in the first column.† Corresponding angles of misorientation and Σ values are given in columns two and three. Figure 1*a* shows the relaxed structure of $\Sigma = 27\,(115)_1$ in projection along the $[1\bar{1}0]$ tilt axis. The triangles and crosses distinguish between the $(2\bar{2}0)$ planes in each crystal period along the tilt axis, and the upper and lower grain coordinate systems are shown in the figure. The shapes drawn into figure 1*a* indicate the atomic groups constituting one period of the boundary. In each period the

TABLE 1

boundary plane	θ/deg	Σ	centred	period vector	structure
$(115)_1/(\bar{1}\bar{1}5)_2$	31.59	27	yes	$\frac{1}{2}[55\bar{2}]_1$	|A.A|
$(3,3,14)_1/(\bar{3},\bar{3},14)_2$	33.72	107	no	$[77\bar{3}]_1$	|AAAAAB|
$(229)_1/(\bar{2}\bar{2}9)_2$	34.89	89	no	$\frac{1}{2}[99\bar{4}]_1$	|AAAB|
$(5,5,21)_1/(\bar{5},\bar{5},21)_2$	37.22	491	yes	$\frac{1}{2}[21,21,\bar{1}0]_1$	|ABABA.ABABA|
$(1,1,4)_1/(\bar{1},\bar{1},4)_2$	38.94	9	no	$[22\bar{1}]_1$	|AB|
$(5,5,19)_1/(\bar{5},\bar{5},19)_2$	40.83	411	yes	$\frac{1}{2}[19,19,\bar{1}0]_1$	|BABAB.BABAB|
$(3,3,11)_1/(\bar{3},\bar{3},11)_2$	42.18	139	yes	$\frac{1}{2}[11,11,\bar{6}]_1$	|BBA.BBA|
$(227)_1/(\bar{2}\bar{2}7)_2$	44.00	57	no	$\frac{1}{2}[77\bar{4}]_1$	|BBBA|
$(113)_1/(\bar{1}\bar{1}3)_2$	50.48	11	yes	$\frac{1}{2}[33\bar{2}]_1$	|B.B|

two triangles, marked t, correspond to tetrahedra seen in projection along an edge. Separating each pair of tetrahedra there are five-sided configurations, marked p, which appear pentagonal in projection although they are not planar. For brevity we call them 'irregular pentagons'. It is important to note that the atomic structure of each half period of the boundary is identical except that atoms represented by triangles in one half correspond to atoms represented by crosses in the other half, and vice versa. Equivalent atoms in each half period are therefore relatively displaced along the tilt axis by $\frac{1}{4}[1\bar{1}0]$. We define the repeat cell of a tilt boundary as the rectangular cell bounded by vectors parallel and perpendicular to the tilt axis with magnitudes equal to the period of the boundary in those two directions. For example, the repeat cell of the $\Sigma = 27\,(115)_1$ boundary is defined by the vectors $\frac{1}{2}[1\bar{1}0]$ and $\frac{1}{2}[55\bar{2}]_1$. The $\Sigma = 27$ c.s.l. unit cell is base-centred orthorhombic and the $(115)_1$ symmetrical tilt boundary is parallel to one of the base-centering faces. Hence the repeat cell of this boundary contains two c.s.l. sites: one shared by the four corners and the second at the centre of the cell. No relaxation can destroy the translational symmetry associated with the c.s.l. in the boundary plane and this is the reason for the equivalence of atoms in each half period. The term 'centred boundary' is used here to connote any tilt boundary that has more than one c.s.l. site in a repeat cell of the boundary. Therefore $\Sigma = 27\,(115)_1$ is centred. However, it is only in $\langle 001\rangle$ and $\langle 110\rangle$ tilt boundaries that the additional c.s.l. sites are at the centre of the repeat cell. For example, in 'centred' $[11\bar{1}]$ tilt boundaries the additional sites are at $\frac{1}{3}[11\bar{1}]$ and $\frac{2}{3}[11\bar{1}]$ along the tilt axis.

Let the repeat cell of a boundary contain s c.s.l. sites. We call a cell that is associated with only one c.s.l. site a primitive cell of the boundary. The area of a primitive cell is thus $1/s$ of the

† The suffixes 1 and 2 signify that the plane, or vector, is expressed in the upper or lower grain coordinate system respectively. If no suffix is used then the plane, or vector, has the same components in both coordinate systems, e.g. $(2\bar{2}0)$.

PHILOSOPHICAL TRANSACTIONS OF THE ROYAL SOCIETY A MATHEMATICAL, PHYSICAL & ENGINEERING SCIENCES

area of a repeat cell. It is convenient, as seen below, to choose the primitive cell bounded by the shortest crystal lattice vector along the tilt axis, and the vector perpendicular to the tilt axis with length $1/s$ times the period of the boundary in that direction. Henceforth this cell will be referred to as the primitive cell of the boundary. Thus the primitive cell of the $\Sigma = 27\,(115)_1$ boundary is

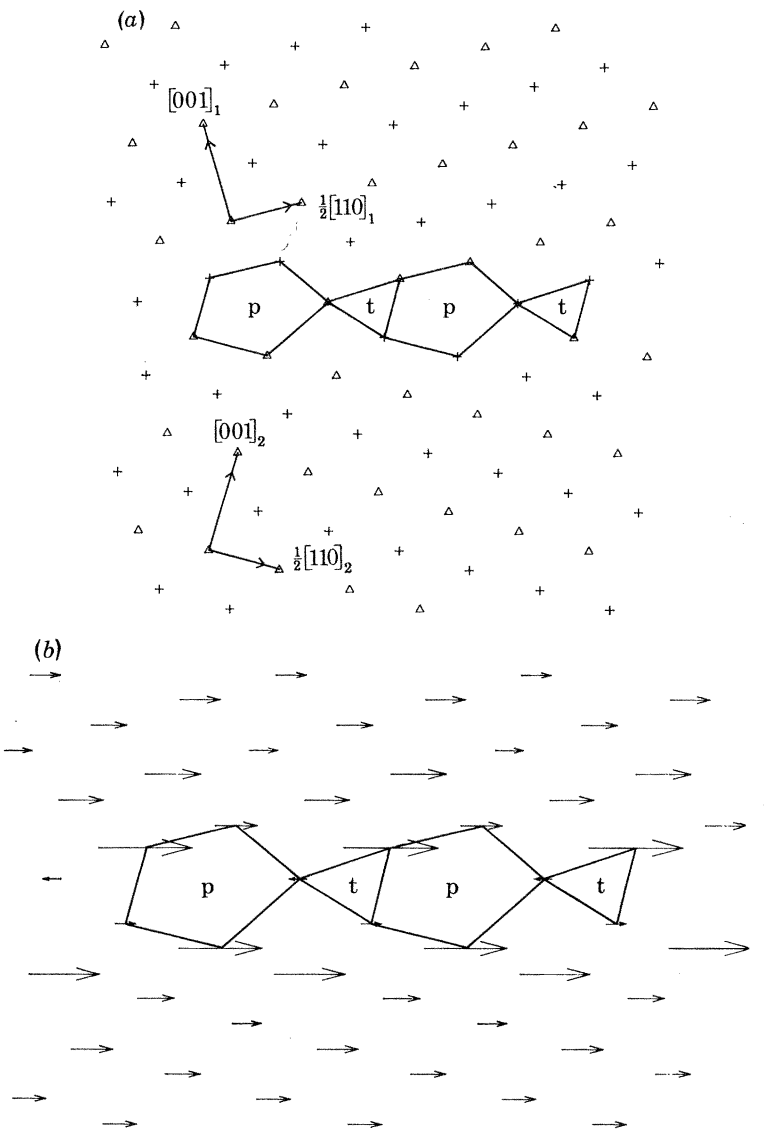

FIGURE 1. (*a*) Relaxed structure of $\Sigma = 27\,(115)_1$, 31.59°/[1$\bar{1}$0] boundary in aluminium; p and t denote irregular pentagons and tetrahedra respectively. (*b*) Corresponding hydrostatic stress field map; arrows pointing to the right/left indicate hydrostatic compression/tension. The middle of each arrow corresponds to an atomic site.

bounded by $\frac{1}{4}[55\bar{2}]_1$ and $\frac{1}{2}[1\bar{1}0]$. We now introduce the concept of a boundary unit. This is a three-dimensional object containing atoms that coincides with a primitive cell in the geometrical boundary plane and, in principle, is of infinite length normal to the boundary plane owing to the absence of translational symmetry in that direction in a bicrystal. For the present purposes it is sufficient to include the smallest possible number of atoms needed to identify the corresponding boundary structure unambiguously. By including more atoms one is only appending relatively

undistorted crystal. The size and shape of a boundary unit in the geometrical boundary plane are prescribed by the primitive cell of the boundary, and are therefore determined entirely by the boundary crystallography. In general, the atomic structure depicted within the unit is expected to vary with the interatomic potential. The atomic structures of all boundary units are identical, but equivalent atoms in adjacent units of a centred boundary are relatively displaced by some multiple of $1/s$ of the shortest crystal vector along the tilt axis.

We define a unit, called A, of the $\Sigma = 27\,(115)_1$ boundary structure shown in figure 1*a* as consisting of one tetrahedron and one of its adjoining irregular pentagons. This unit is bounded by $\frac{1}{4}[55\bar{2}]_1$ and $\frac{1}{2}[1\bar{1}0]$ as required, and contains sufficient atoms to typify the boundary structure. The boundary structure may be represented by |A.A| (as shown in column 6 of table 1), where the bars denote one period of the boundary perpendicular to the tilt axis, and the dot signifies that equivalent atoms in adjacent units are relatively displaced by $\frac{1}{4}[1\bar{1}0]$ along the tilt axis. |A.A| is called the unit representation of this boundary structure. For the same interatomic potential and tilt axis, units of boundaries with different misorientations may be distinguished by the vectors bounding the primitive cells perpendicular to the tilt axis. It may be said that these vectors characterize the boundary units. Thus $\frac{1}{4}[55\bar{2}]_1$ characterizes the unit of the $\Sigma = 27\,(115)_1$ boundary in this series of $[1\bar{1}0]$ tilt boundaries.

Figure 1*b* shows the hydrostatic stress field map of the $\Sigma = 27\,(115)_1$ boundary. The equivalence of atoms in each half period is clearly revealed in figure 1*b* because exactly the same hydrostatic stress exists at equivalent sites. For example, compare the hydrostatic stresses at corresponding apices of the two tetrahedra shown as triangles. From Frank's formula we see that each A unit may be associated with a [001] lattice dislocation. However, since the spacing of these dislocations is only $\frac{1}{4}|[55\bar{2}]_1|$ it is perhaps more meaningful to describe the boundary as dislocation free, corresponding to the simple shear description of the relation between the crystal lattices.

It can be shown (Sutton 1981) that all (hhk) $[1\bar{1}0]$ symmetrical tilt boundaries in f.c.c. crystals are centred provided both h and k are odd. Figure 2*a* shows the relaxed structure of the $\Sigma = 11\,(113)_1$ boundary. Two capped trigonal prisms (c.t.ps) composing one period of this boundary are outlined by broken lines. This boundary is centred and hence the c.t.ps are identical except for a relative displacement of $\frac{1}{4}[1\bar{1}0]$ along the tilt axis. We may conveniently define a unit, B, of this boundary as one c.t.p. Each B unit is then bounded by $\frac{1}{2}[1\bar{1}0]$ and $\frac{1}{4}[33\bar{2}]$ in the boundary plane as required, and the structure of the boundary may be represented by |B.B|. B units are characterized by $\frac{1}{4}[33\bar{2}]$. The hydrostatic stress field map of this boundary is shown in figure 2*b*, Again we can formally associate a [001] lattice dislocation with each B unit, and it is noted that the core structure of each dislocation has changed from an A unit to a B unit. However, since the spacing of these dislocations is only *ca.* 1.173*a* it is again preferable to describe the bicrystal as a simple shear on the boundary plane.

The relaxed structure of the $\Sigma = 107\,(3, 3, 14)_1$ boundary is shown in figure 3*a*. Each period of this boundary is composed of five slightly distorted A units, shown by full lines, and one slightly distorted B unit, shown by broken lines. Hence this boundary structure may be represented by |AAAAAB|, as indicated in table 1. We call the vector bounding the repeat cell of a boundary that is perpendicular to the tilt axis the period vector. In this case the period vector is $[77\bar{3}]_1$. The decomposition of the structure of each period of this boundary into five A units and one B unit may be expressed as a vectorial decomposition of the period vector:

$$[77\bar{3}]_1 = \tfrac{5}{4}[55\bar{2}]_1 + \tfrac{1}{4}[33\bar{2}]_1.$$

PHILOSOPHICAL TRANSACTIONS OF THE ROYAL SOCIETY A MATHEMATICAL, PHYSICAL & ENGINEERING SCIENCES

This equation reflects the filling of the $(3, 3, 14)_1$ boundary period by five A units and one B unit because of our choice of primitive cells with sides parallel and perpendicular to the tilt axis. However, in §6 it is shown that different boundary units cannot be combined in this manner if they have incompatible translation states. Within each period of the $\Sigma = 107$ boundary, the local rotation of $(115)_1$ and $(\bar{1}\bar{1}5)_2$ planes, to make them parallel to the boundary plane at A

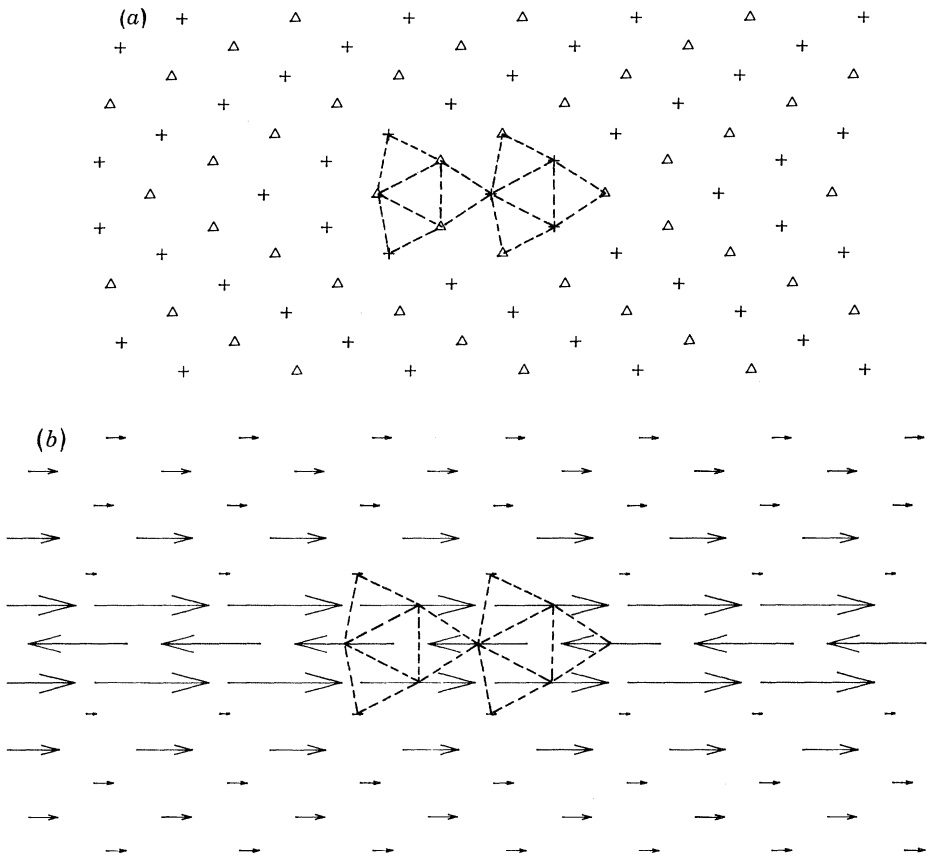

FIGURE 2. (*a*) Relaxed structure of $\Sigma = 11\ (113)_1$, $50.48°/[1\bar{1}0]$ boundary in aluminium; the two capped trigonal prisms in one boundary period are indicated by broken lines. (*b*) Corresponding hydrostatic stress field map.

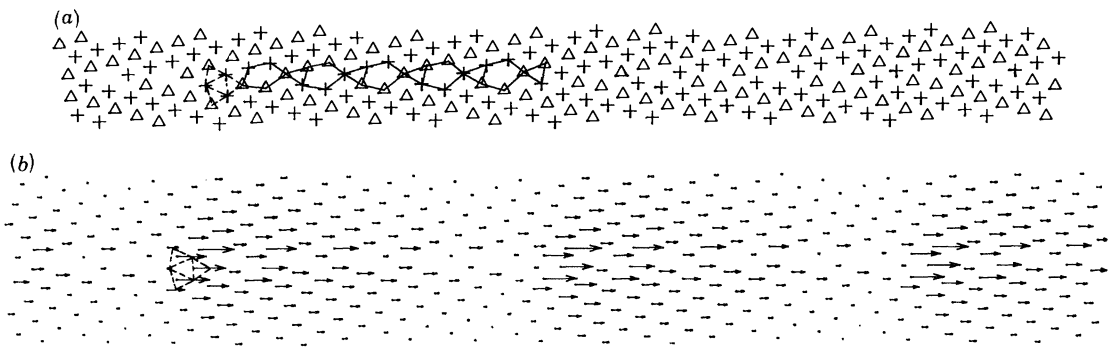

FIGURE 3. (*a*) Relaxed structure of $\Sigma = 107\ (3, 3, 14)_1$, $33.72°/[1\bar{1}0]$ boundary in aluminium; the five A units and one B unit in one period of the boundary are indicated by full and broken lines respectively. (*b*) Corresponding hydrostatic stress field map.

PHILOSOPHICAL TRANSACTIONS OF THE ROYAL SOCIETY A MATHEMATICAL, PHYSICAL & ENGINEERING SCIENCES

units, creates an incompatability between A and B units perpendicular to the boundary plane. This incompatability results in an intrinsic edge dislocation at each B unit with Burgers vector equal to $\frac{2}{27}[115]_1$. This Burgers vector can be verified by using Frank's formula since the dislocations are spaced by $|[77\bar{3}]|$ and the angular deviation from the $\Sigma = 27\,(115)_1$ misorientation is arccos (2887/2889). The creation of each $\frac{2}{27}[115]_1$ dislocation may be viewed as a consequence of the minimization of the deviations of the local misorientation across the boundary at each unit from the ideal state of the unit. The physical significance of this secondary g.b.d. description is determined by the degree to which the dislocations are localized and distinguishable, which in turn depends on the existence of local misorientation differences between A and B units. That the secondary g.b.ds are indeed localized is evidenced by the hydrostatic stress field map, figure 3*b*. The stress field consists of a superposition of the field of the $\Sigma = 27\,(115)_1$ boundary (figure 1*b*) and the field of the array of uniformly spaced $\frac{2}{27}[115]_1$ g.b.ds. Between successive B units (shown by dashed lines) there is a gradual increase in overall compression to a maximum at each B unit followed by an abrupt transition to relative tension. This indicates that an edge dislocation is indeed located at each B unit, and the sharpness of the transition demonstrates that each of these dislocations is well localized and distinct.

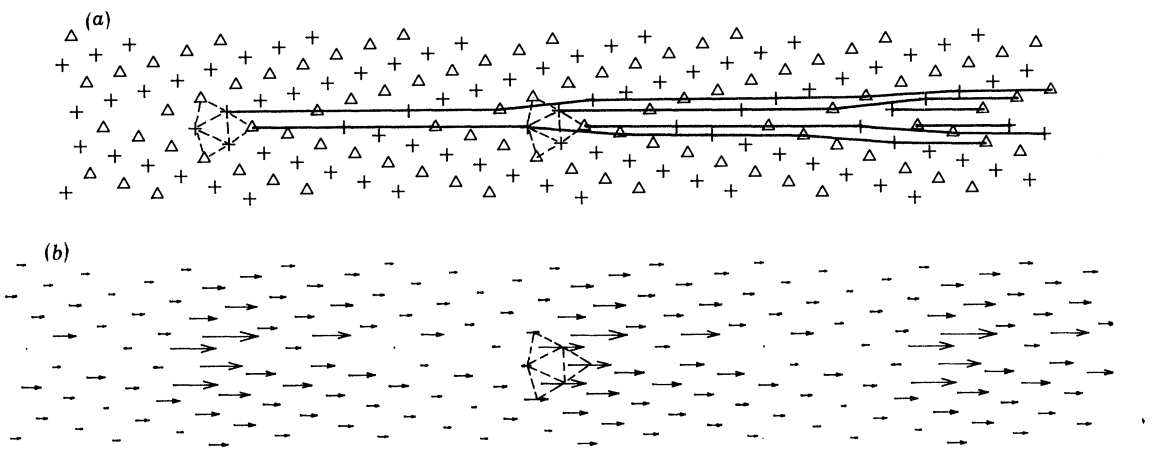

FIGURE 4. (*a*) Relaxed structure of $\Sigma = 89\,(229)_1$, 34.89°/$[1\bar{1}0]$ boundary in aluminium. The two B units, shown by broken lines, are separated by one period of the boundary. Full lines show $(115)_1$ and $(\bar{1}\bar{1}5)_2$ planes entering and terminating in the boundary at B units. (*b*) Corresponding hydrostatic stress field map.

Figures 4*a*, *b* show the relaxed structure and hydrostatic stress field map of the $\Sigma = 89\,(229)_1$ boundary. B units, indicated by broken lines, are separated by one period of the boundary. Three A units may be seen between each pair of B units and hence the unit representation of this boundary is |AAAB|. The period vector, $\frac{1}{2}[99\bar{4}]_1$, undergoes the following decomposition:

$$\tfrac{1}{2}[99\bar{4}]_1 = \tfrac{3}{4}[55\bar{2}]_1 + \tfrac{1}{4}[33\bar{2}]_1.$$

Full lines in figure 4*a* show $(115)_1$ and $(\bar{1}\bar{1}5)_2$ planes entering the boundary in pairs at B units and terminating parallel to the boundary at the next B unit. This indicates that each B unit is located at the core of an edge dislocation with Burgers vector magnitude equal to twice the {115} interplanar spacing. Moreover, since the direction of the Burgers vector is perpendicular to $(115)_1$ and $(\bar{1}\bar{1}5)_2$ the Burgers vector is $\frac{2}{27}[115]_1$. This Burgers vector is twice a primitive d.s.c. dislocation of the $\Sigma = 27$ coincidence system. Since the angle of misorientation of the $\Sigma = 89$ boundary is greater than that of the $\Sigma = 27$ boundary we have chosen the positive sign for the

Burgers vector. The structure of the $\Sigma = 89\,(229)_1$ boundary may therefore be described as that of the $\Sigma = 27\,(115)_1$ boundary with a superimposed array of uniformly spaced $\frac{2}{27}[115]_1$ intrinsic secondary g.b.ds whose cores correspond to units from the $\Sigma = 11\,(113)_1$ boundary. This description is consistent with figure 4*b* where each B unit, identified by broken lines, coincides with a sharp transition from maximum compression to relative tension. Furthermore, the compressive side of the B unit corresponds to the side at which two {115} planes terminate.

Figures 5*a*, *b* show the relaxed structure and hydrostatic stress field map of the $\Sigma = 491\,(5, 5, 21)_1$ boundary. This boundary is centred and each half period has the structure BAABA so that the boundary structure is represented by |BAABA.BAABA|. The period vector is $\frac{1}{2}[21, 21, \overline{10}]_1$ and the decomposition of each half of this vector is as follows:

$$\tfrac{1}{4}[21, 21, \overline{10}]_1 = \tfrac{3}{4}[55\overline{2}]_1 + \tfrac{2}{4}[33\overline{2}]_1.$$

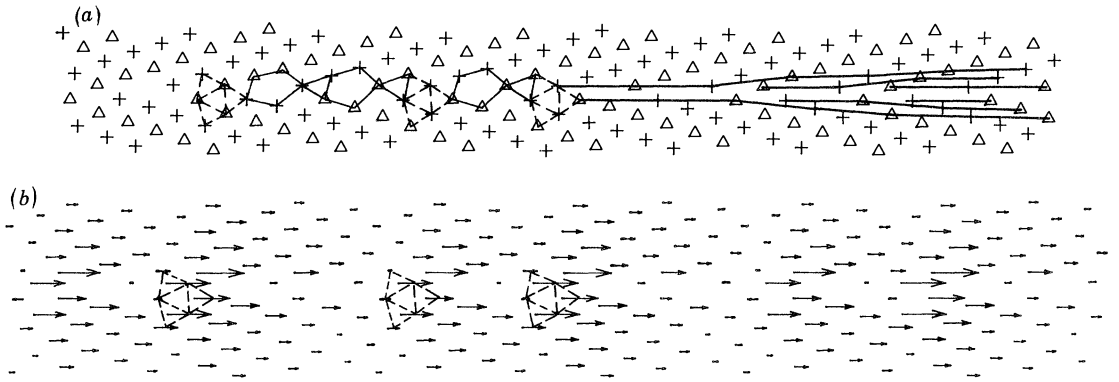

FIGURE 5. (*a*) Relaxed structure of $\Sigma = 491\,(5, 5, 21)_1$, 37.22°/[1$\overline{1}$0] boundary in aluminium. B units (broken lines) are separated alternately by two and one A units (full lines). Full lines outline $(115)_1$ and $(\overline{11}5)_2$ planes entering and terminating in the boundary at B units. (*b*) Corresponding hydrostatic stress field map.

Pairs of $(115)_1$ and $(\overline{11}5)_2$ planes are shown in figure 5*a* entering and terminating in the boundary at B units. In this case the B units are spaced by either one or two A units and thus the corresponding $\frac{2}{27}[115]_1$ dislocations are also non-uniformly spaced. In figure 5*b* the stress fields of distinct edge dislocations are located at B units confirming that this secondary dislocation description is physically significant.

The relaxed structure and hydrostatic stress field map of the $\Sigma = 9\,(114)_1$ boundary are shown in figures 6*a*, *b*. Each period of the boundary is composed of one A unit, shown by full lines, and one B unit, shown by broken lines, and the boundary structure is therefore represented by |AB|. The decomposition of the period vector is as follows:

$$[22\overline{1}]_1 = \tfrac{1}{4}[55\overline{2}]_1 + \tfrac{1}{4}[33\overline{2}]_1.$$

Figure 6*b* indicates that an edge dislocation exists in each period of the boundary but since there is an equal number of A and B units either of them may be regarded as the preserved reference structure. Thus there is an ambiguity in the choice of the most suitable reference structure for describing the secondary g.b.d. content of the boundary.

Figures 7*a*, *b* show the relaxed structure and hydrostatic stress field map of the $\Sigma = 411\,(5, 5, 19)_1$ boundary. Each half period of this centred boundary is composed of two A units, shown by full lines, and three B units, shown by dashed lines. The unit representation of this boundary is |ABABB.ABABB|. The decomposition of each half-period vector is as follows:

$$\tfrac{1}{4}[19, 19, \overline{10}]_1 = \tfrac{3}{4}[33\overline{2}]_1 + \tfrac{2}{4}[55\overline{2}]_1.$$

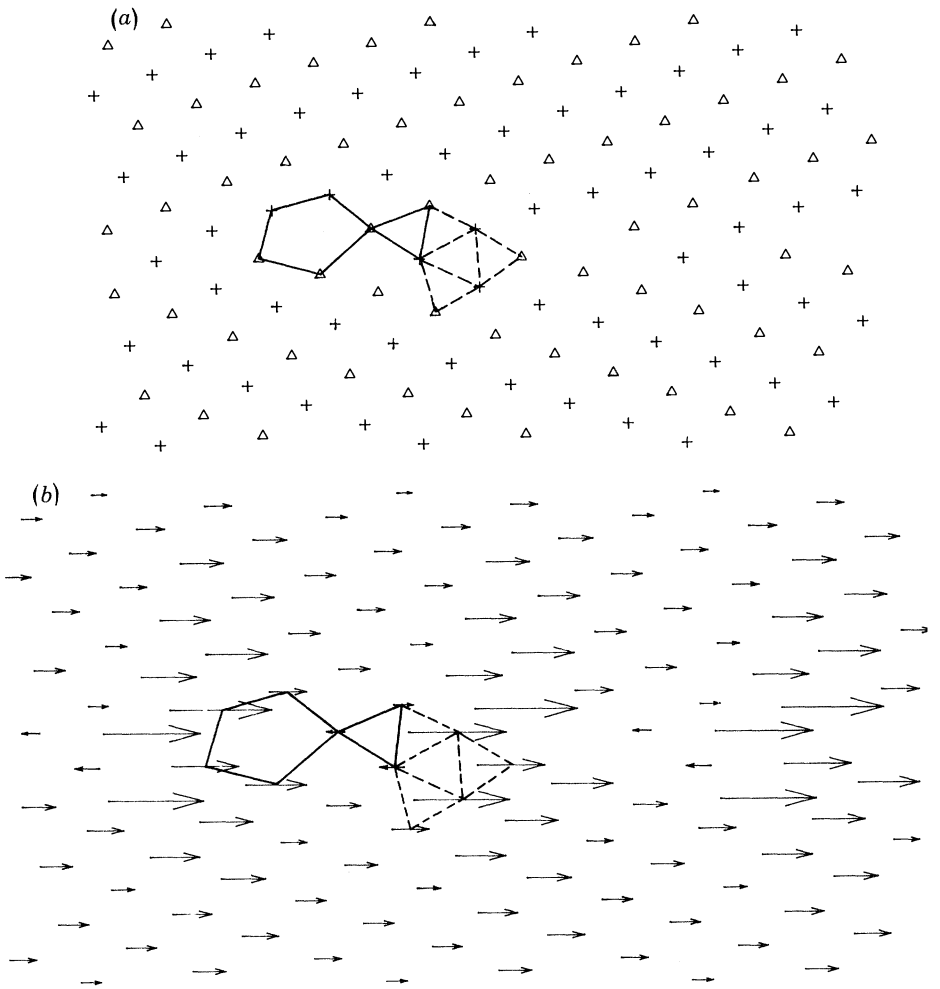

FIGURE 6. (*a*) Relaxed structure of $\Sigma = 9\ (114)_1$, 38.94°/[1$\bar{1}$0] boundary in aluminium. One A and one B unit, composing one period of the boundary, are shown by full and broken lines respectively. (*b*) Corresponding hydrostatic stress field map.

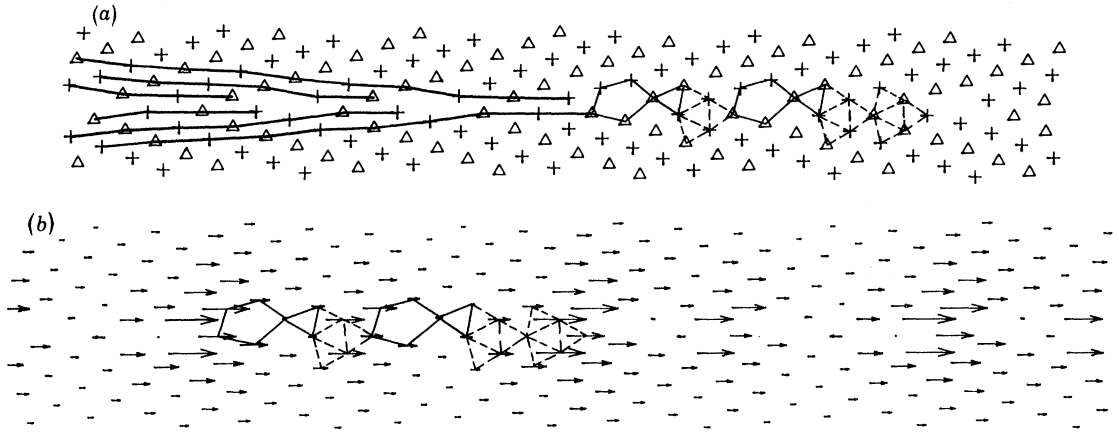

FIGURE 7. (*a*) Relaxed structure of $\Sigma = 411\ (5, 5, 19)_1$, 40.83°/[1$\bar{1}$0] boundary in aluminium. Two A units and three B units, composing one half period of the boundary, are shown by full and broken lines respectively. Pairs of $(113)_1$ and $(\bar{1}\bar{1}3)_2$ planes are shown entering and terminating in the boundary at A units. (*b*) Corresponding hydrostatic stress field map.

Figure 7*b* indicates an array of non-uniformly spaced edge g.b.ds and since there are now more B than A units, $\Sigma = 11\,(113)_1$ is the preserved reference structure. Pairs of $(113)_1$ and $(\bar{1}\bar{1}3)_2$ planes are shown in figure 7*a* entering the boundary at A units and terminating at the next A unit. Thus A units are now identified with the cores of $-\frac{2}{11}[113]_1$ dislocations. Their Burgers vectors are twice primitive d.s.c. vectors of the $\Sigma = 11$ coincidence system.

Table 1 indicates that the remaining boundaries in this series are also composed of A and B units with B units in the majority. In each case A units are located at the cores of $-\frac{2}{11}[113]_1$ dislocations preserving the $\Sigma = 11\,(113)_1$ structure. As a final example, figures 8*a*, *b* show the

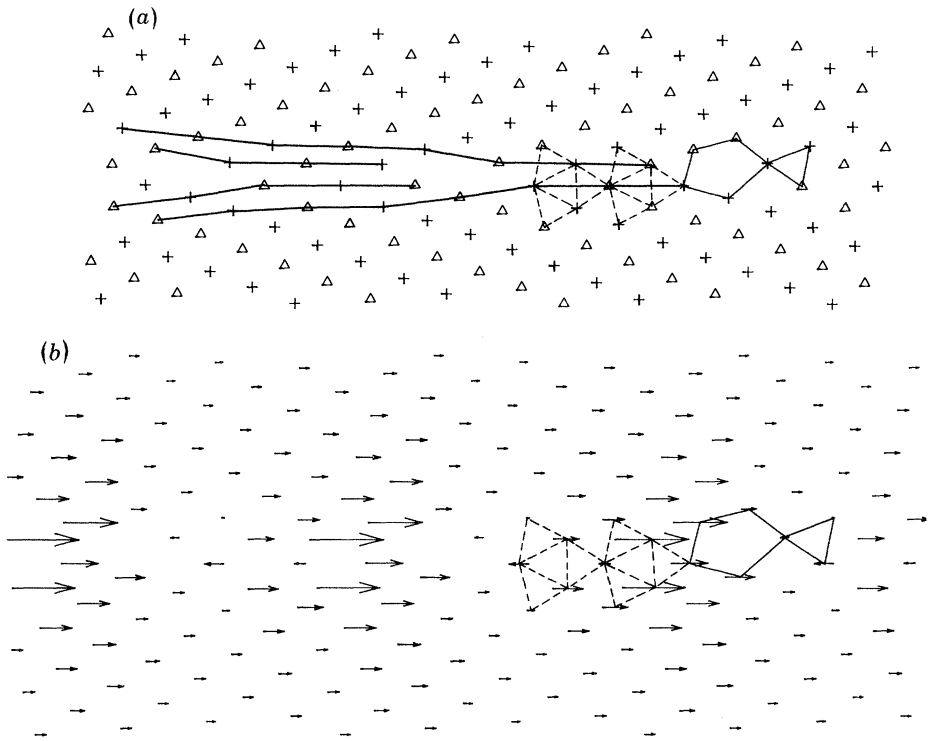

FIGURE 8. (*a*) Relaxed structure of $\Sigma = 139\ (3, 3, 11)_1$, 42.18°/[1$\bar{1}$0] boundary in aluminium. Two B units and one A unit, composing one half period of the boundary, are shown by broken and full lines respectively. Pairs of $(113)_1$ and $(\bar{1}\bar{1}3)_2$ planes are shown entering and terminating in the boundary at A units. (*b*) Corresponding hydrostatic stress field map.

relaxed structure and hydrostatic stress field map of $\Sigma = 139\,(3, 3, 11)_1$. Each half period of this centred boundary is composed of two B units, shown by dashed lines, and one A unit, shown by full lines. In figure 8*a* it is seen that pairs of $(113)_1$ and $(\bar{1}\bar{1}3)_2$ planes enter the boundary and terminate at A units. These plane terminations correspond to the transition from maximum compression to relative tension seen at A units in figure 8*b*.

4.3. *Analysis of the results for* $31.59 \leqslant \theta \leqslant 50.48°$

All of the calculated boundary structures are composed of A and B units. A and B units are therefore the fundamental structural elements of all these boundary structures and hence $\Sigma = 27\,(115)_1$ and $\Sigma = 11\,(113)_1$ are adjacent favoured boundaries. The hydrostatic stress field maps reveal arrays of discrete, localized edge g.b.ds in all the calculated structures of the inter-

vening non-favoured boundaries. The source of each of those edge g.b.ds is the incompatibility, normal to the boundary plane, created by the local misorientation differences across A and B units. Since there are no incompatibilities between adjacent units in favoured boundaries they are the appropriate reference structures for describing the intrinsic secondary g.b.d. structures of intervening non-favoured boundaries. Between the $\Sigma = 27$ and $\Sigma = 9$ orientations there are more A than B units in the boundary structures and B units are then located at the cores of $\frac{2}{27}[115]_1$ intrinsic d.s.c. dislocations preserving the $\Sigma = 27\,(115)_1$ reference boundary structure. Similarly, between the $\Sigma = 9$ and $\Sigma = 11$ orientations there are more B than A units, and A units are then located at the cores of $-\frac{2}{11}[113]_1$ intrinsic d.s.c. dislocations preserving the $\Sigma = 11$ $(113)_1$ reference boundary structure. The $\Sigma = 9\,(114)_1$ boundary is composed of an equal number of A and B units. At this boundary both secondary g.b.d. descriptions apply, and the change from one description to the other occurs at this boundary misorientation ($\theta = 38.94°$). It is remarkable that these secondary g.b.d. descriptions retain physical significance throughout their respective misorientation ranges.

The unit of a favoured boundary is a fundamental structural element, i.e. it is not composed of units from any other boundaries. If we choose to describe a favoured boundary as an array of uniformly spaced lattice dislocations, accommodating the misorientation from the ideal lattice, then each unit of a favoured boundary is associated with one lattice dislocation. Owing to their small spacing, the stress fields of these lattice dislocations are no longer distinguishable and the dislocation core structures differ in different favoured boundaries. Despite the limited physical significance of this description it is interesting to note that a non-favoured boundary may be regarded as an array of non-uniformly spaced lattice dislocations. The irregularities in the lattice dislocation spacing are located at minority units and therefore coincide with secondary dislocations based on the majority unit reference structure. For example, consider $\Sigma = 89\,(229)_1$, whose unit representation is |AAAB|. All four units in each period may be regarded as cores of [001] lattice dislocations, the three A units with spacing $\frac{1}{4}|[55\bar{2}]_1|$ and the B unit with 'spacing' $\frac{1}{4}|[33\bar{2}]_1|$. Thus each B unit is an irregularity in the spacing of [001] lattice dislocations in this boundary, where the regular spacing is defined as that of the $\Sigma = 27\,(115)_1$ favoured boundary, i.e. $\frac{1}{4}|[55\bar{2}]_1|$. On the other hand each B unit corresponds to the core of a $\frac{2}{27}[115]_1$ secondary dislocation preserving the $\Sigma = 27\,(115)_1$ favoured boundary structure. Secondary dislocations based on some favoured boundary reference structure are therefore formally equivalent to irregularities in the spacing of primary dislocations composing that favoured boundary (see also Read & Shockley 1950, Balluffi 1980). It is notedthat the Burgers vectors, $\frac{2}{27}[115]_1$ and $-\frac{2}{11}[113]_1$ of the secondary dislocations preserving the above favoured boundaries are non-primitive d.s.c. vectors. The primitive d.s.c. dislocations, $\frac{1}{27}[115]_1$ and $-\frac{1}{11}[113]_1$, are associated with large steps in the $\Sigma = 27\,(115)_1$ and $\Sigma = 11\,(113)_1$ boundaries, respectively. From the present calculations it appears that it is always energetically more favourable to have an array of non-primitive dislocations without steps, than it is to have an array of primitive dislocations with steps that may possess a lower elastic strain field energy. Presumably if the dislocation spacing, d, were sufficiently large then primitive dislocations with steps would become energetically favourable. However, King & Smith (1980) considered the case of an array of $\frac{2}{11}[113]_1$ dislocations superimposed on $\Sigma = 11\,(113)_1$ boundary and estimated that $d > 100$ nm is necessary for the formation of primitive dislocations to be favourable. Considerably larger spacings are expected for an array of $\frac{2}{27}[115]_1$ dislocations superimposed on $\Sigma = 27\,(115)_1$ boundary. Therefore, it is reasonable to assume that the above primitive d.s.c. dislocations do not occur in boundaries in the range $31.59 \leqslant \theta \leqslant 50.48°$.

PHILOSOPHICAL TRANSACTIONS OF THE ROYAL SOCIETY A MATHEMATICAL, PHYSICAL & ENGINEERING SCIENCES

This is important because if steps did occur in the boundary then it would no longer be composed only of A and B units.

An important result of the calculations is that the boundary structures were found to vary continuously with misorientation. Continuity of boundary structure between A and B favoured boundaries entails that all boundaries are composed of A and B units and furthermore the sequence of A and B units is strictly continuous with that of neighbouring boundaries in the misorientation range. We shall explain what this means by considering a specific example. Consider $\Sigma = 491\,(5, 5, 21)_1$, which is a centred boundary; we know that each half period is composed of three A units and two B units. However, suppose the sequence of A and B units in this boundary were not known. It is only necessary to consider one sequence of five units because of the periodicity in the boundary. Furthermore, a cyclic interchange of units throughout the boundary only displaces the origin and does not change the boundary structure. Therefore, there are $5!/(5 \times 3! \times 2!) = 2$ non-equivalent sequences: (i) ...BAAAB... and (ii) ...BABAA.... We shall show that only the second possibility is continuous with neighbouring boundary structures. For brevity, if each repeat sequence of units of a boundary consists of m A units and n B units we call the boundary the $m{:}n$ boundary. Thus $\Sigma = 491\,(5, 5, 21)_1$ is the 3:2 boundary. The 3:2 boundary has a misorientation between those of the 1:1 and 2:1 boundaries, whose structures can only be ...AB... and ...AAB... respectively. In both 1:1 and 2:1 boundaries every B unit is sandwiched between A units. This is true of the second possibility for the 3:2 boundary, but not the first. Hence the sequence of units in the second possibility is continuous with the sequences in neighbouring boundaries but the first possibility is not. The second possibility is, indeed, found by direct calculation, as may be seen in figure 5*a*. To obtain the second sequence for the 3:2 boundary from the known 1:1 and 2:1 sequences it is only necessary to write

$$\mathrm{BA} + \mathrm{BAA} = \mathrm{BABAA} \quad \text{or} \quad \mathrm{AB} + \mathrm{AAB} = \mathrm{ABAAB},$$

i.e. continuity is assured provided one writes both 1:1 and 2:1 components beginning with the same unit. Note that continuity of boundary structure results in the maximum possible separation of secondary dislocations based on the appropriate favoured boundary reference structure.

The number, R, of non-equivalent periodic boundary structures that may be obtained from m A units and n B units is given by

$$R = (m+n-1)!/m!n!.$$

For example, when $m = 12$ and $n = 11$ we obtain $R = 58\,786$. All of these structures lead to the same macroscopic boundary misorientation. The significance of continuity of boundary structure is that it is satisfied only by one of the R possibilities and that is the structure found by direct calculation. We now give an example to show how to predict the structure of a very high Σ boundary using the principle of continuity of boundary structure. Consider the structure of $\Sigma = 1881\,(10, 10, 41)_1$, $38.06°/[1\bar{1}0]$ in aluminium. This boundary is composed of some mixture of the above A and B units. The boundary is not centred and therefore the repeat sequence of units fills one period of the boundary. Let the numbers of A and B units in one period be m and n respectively. The period vector undergoes the following decomposition:

$$\tfrac{1}{2}[41, 41, \overline{20}]_1 = \tfrac{1}{4}m[55\bar{2}]_1 + \tfrac{1}{4}n[33\bar{2}]_1.$$

Solving this equation we find $m = 11$ and $n = 9$ (for which $R = 8398$). The structure of the 11:9 boundary must be continuous with the structures of 1:1 and 2:1 boundaries, which can

only be ...AB... and ...AAB... respectively. Starting from the known 1:1 and 2:1 sequences the 11:9 sequence is constructed by forming successively closer approximations:

$$2:1+1:1=3:2,$$

i.e. $$\mathrm{AAB}+\mathrm{AB}=\mathrm{AABAB};$$

$$3:2+1:1=4:3,$$

i.e. $$\mathrm{AABAB}+\mathrm{AB}=\mathrm{AABABAB};$$

$$4:3+1:1=5:4,$$

i.e. $$\mathrm{AABABAB}+\mathrm{AB}=\mathrm{AABABABAB};$$

$$2(5:4)+1:1=11:9,$$

i.e. $$2\,(\mathrm{AABABABAB})+\mathrm{AB}=\mathrm{AABABABABAABABABABAB}.$$

Provided all boundaries in the misorientation range between two favoured boundaries are composed of units from the favoured boundaries, it is possible to derive the unit representation of any boundary in that misorientation range, by using the principle of continuity of boundary structure. The unit representation provides, at least qualitatively, the atomic structure and stress field of the boundary. While one cannot explicitly calculate the structure of every boundary in the range $31.59 \leqslant \theta \leqslant 50.48°$, to prove that all boundaries in this range are composed of A and B units, the above calculations suggest no reason for believing otherwise. Furthermore, it is shown in part III that all boundaries in this range certainly can be constructed from A and B units.

4.4. *Boundaries in the misorientation range* $0 \leqslant \theta \leqslant 31.59°$

Table 2 lists the parameters of boundaries selected in this misorientation range. As may be seen in column six of this table all of the calculated boundary structures are composed of two units, A and C. The A units are the same as before and belong to the $\Sigma = 27\,(115)_1$ favoured boundary. The C units belong to the ideal crystal. As θ approaches zero the boundary plane tends to (001) and the period vector tends to the [110] direction. The next favoured 'boundary' is thus $\Sigma = 1\,(001)$ and the appropriate primitive cell is bounded by $\frac{1}{2}[110]$ and $\frac{1}{2}[1\bar{1}0]$. A suitable choice of C unit, which is bounded by these $\frac{1}{2}\langle 110\rangle$ vectors in the (001) plane, is indicated in figure 9 by broken lines. Since all of the calculated structures are composed of A and C units it is reasonable to assume that all boundaries in this misorientation range are composed of these units and therefore that continuity of boundary structure exists throughout the range. We therefore present here only one of the calculated structures. Figures 10*a*, *b* show the relaxed structure and hydrostatic stress field map of $\Sigma = 129\,(2, 2, 11)_1$. Each period of the boundary is composed of four A units and one C unit, shown by dashed lines. The unit representation of the boundary structure is therefore |AAAAC|. The period vector, $\frac{1}{2}[11, 11, \bar{4}]_1$, undergoes the following decomposition: $\frac{1}{2}[11, 11, \bar{4}]_1 = \frac{4}{4}[55\bar{2}]_1 + \frac{1}{2}[110]_1$.

TABLE 2

boundary plane	θ/deg	Σ	centred	period vector	structure
$(001)_1/(001)_2$	0	1	no	$\frac{1}{2}[110]_1$	|C|
$(1, 1, 13)_1/(\bar{1}, \bar{1}, 13)_2$	12.42	171	yes	$\frac{1}{2}[13, 13, \bar{2}]_1$	|CCCCA.CCCCA|
$(117)_1/(\bar{1}\bar{1}7)_2$	22.84	51	yes	$\frac{1}{2}[77\bar{2}]_1$	|CA.CA|
$(116)_1/(\bar{1}\bar{1}6)_2$	26.53	19	no	$[33\bar{1}]_1$	|CAA|
$(2, 2, 11)_1/(\bar{2}, \bar{2}, 11)_2$	28.84	129	no	$\frac{1}{2}[11, 11, \bar{4}]_1$	|CAAAA|
$(3, 3, 16)_1/(\bar{3}, \bar{3}, 16)_2$	29.70	137	no	$[88\bar{3}]_1$	|CAAAAAA|
$(115)_1/(\bar{1}\bar{1}5)_2$	31.59	27	yes	$\frac{1}{2}[55\bar{2}]_1$	|A.A|

The C units identified in figure 10*a* are a somewhat distorted form of the perfect C unit shown in figure 9. The C unit distortion decreases as θ approaches zero while, at the same time, the distortion of A units increases. By distortion of a favoured boundary unit we mean only the change in interatomic separation between the same atoms defining the unit in its ideal state, i.e. addition or removal of atoms to the unit is not permissible. This distortion is regarded as

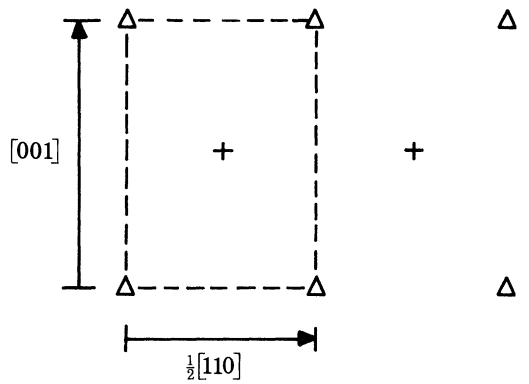

FIGURE 9. [1$\bar{1}$0] Projection of ideal f.c.c. crystal with a C unit outlined by broken lines.

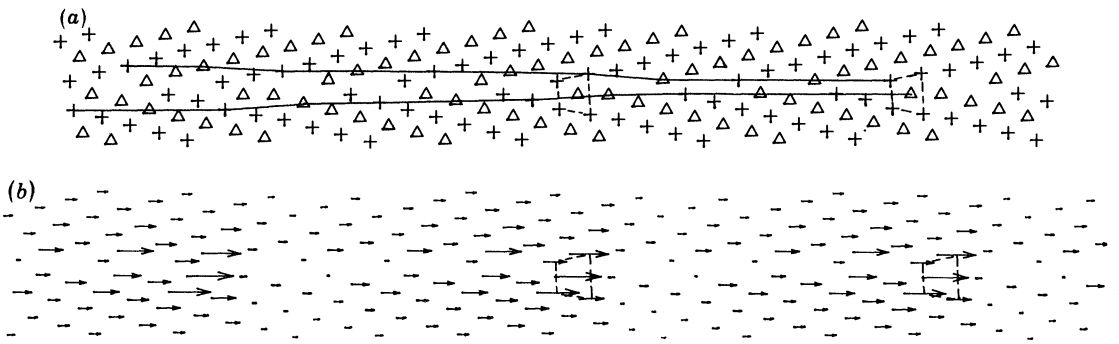

FIGURE 10. (*a*) Relaxed structure of $\Sigma = 129\,(2, 2, 11)_1$, 28.48°/[1$\bar{1}$0] boundary in aluminium. Two C units, separated by one period of the boundary, are shown by broken lines. A pair of $(115)_1$ and $(\bar{1}\bar{1}5)_2$ planes is shown entering the boundary at one C unit and terminating at the next. (*b*) Corresponding hydrostatic stress field map.

acceptable if the distortions of similar units in nearby non-favoured boundaries decrease smoothly to zero as the misorientation of the corresponding favoured boundary is approached. The distorted C units of figure 10*a* are not parts of units from another favoured boundary. Between successive $(115)_1$ and $(\bar{1}\bar{1}5)_2$ terminations (shown by full lines in figure 10*a*) there are four A units so that the remainder of each period of the $(2, 2, 11)_1$ boundary can only be filled by a unit characterized by $\frac{1}{2}[110]$. Figure 10*b* also indicates that between successive alternations from maximum compression to relative tension there are four A units.

It is consistent with figure 10*b* to regard C units as the cores of $-\frac{2}{27}[115]_1$ d.s.c. dislocations preserving the $\Sigma = 27\,(115)_1$ favoured boundary. In the range $0 < \theta \leqslant 22.84°$ minority units are A type and it is then consistent with the stress field maps and Frank's formula to regard A units as the cores of [001] lattice dislocations preserving the (001) plane of the ideal crystal. The $\Sigma = 51\,(117)_1$ ($\theta = 22.84°$) boundary is where the (001) plane of the ideal crystal and the

$\Sigma = 27\,(115)_1$ boundary are equally suitable reference structures because the $(117)_1$ boundary is composed of an equal number of A and C units:

$$\tfrac{1}{4}[55\bar{2}]_1 + \tfrac{1}{2}[110]_1 = \tfrac{1}{4}[77\bar{2}]_1$$

where $\frac{1}{4}[77\bar{2}]_1$ is half the period vector of this centred boundary. It is noted that the cores of $-\frac{2}{27}[115]_1$ dislocations contain C units while the cores of $+\frac{2}{27}[115]_1$ dislocations contain B units. Thus, although the magnitudes of the Burgers vectors of these dislocations are the same, their structures are different. This result may be rationalized by symmetry considerations. In general, there is no symmetry operation of the holosymmetric point group of a symmetrical tilt boundary that can generate an edge g.b.d. with Burgers vector $-\boldsymbol{b}$ from one with $+\boldsymbol{b}$, if $\boldsymbol{b}$ is perpendicular to the boundary plane and the dislocation line is parallel to the tilt axis. Therefore, in general, there is no reason to expect the core structures of such dislocations to be identical. A full symmetry analysis of equivalent g.b.d. core structures in tilt boundaries has been made by Sutton (1981).

5. [001] Symmetrical tilt boundaries in copper

Table 3 summarizes the parameters of boundaries selected for this study. For reasons of space, only two of the calculated structures are shown here. The last column of table 3 shows the unit representations of the calculated boundary structures. The boundary misorientations were defined with respect to the (110) plane of the ideal crystal. Thus as $\theta \to 0$ the boundary planes tend to (110) and the period vector tends to the $[\bar{1}10]$ direction. Clearly, the (110) plane of the ideal crystal is a favoured 'boundary' of this series. The appropriate primitive cell of the (110) plane is bounded by [001] and $\frac{1}{2}[\bar{1}10]$, and we call a unit of this plane A. Figure 11 shows a [001] projection of the ideal crystal and an A unit is outlined by broken lines; it is characterized by the vector $\frac{1}{2}[\bar{1}10]$. It can be shown that $(hk0)_1/[001]$ symmetrical tilt boundary is centred provided h and k are mixed odd and even. Equivalent atoms in adjacent units of centred [001] tilt boundaries are relatively displaced by $\frac{1}{2}[001]$ along the tilt axis.

Table 3

boundary plane	θ/deg	Σ	γ/(mJ/m^2)	centred	period vector	structure
$(110)_1/(110)_2$	0	1	0	no	$\frac{1}{2}[\bar{1}10]_1$	|A|
$(540)_1/(450)_2$	12.68	41	770	yes	$[\bar{4}50]_1$	|AAAB.AAAB|
$(750)_1/(570)_2$	18.92	37	980	no	$\frac{1}{2}[\bar{5}70]_1$	|AABAB|
$(530)_1/(350)_2$	28.07	17	1161	no	$\frac{1}{2}[\bar{3}50]_1$	|ABB|
$(210)_1/(120)_2$	36.87	5	1194	yes	$[\bar{1}20]_1$	|B.B|

Figures 12*a*, *b* show the relaxed structure and hydrostatic stress field map of the $\Sigma = 5\,(210)_1$ boundary. The coordinate system used throughout this [001] symmetrical tilt boundary study is displayed in figure 12*a*. Using the same potential for copper, Crocker & Faridi (1980) have also obtained this boundary structure. We shall show that this is a favoured boundary. Because it is centred its unit is characterized by $\frac{1}{2}[\bar{1}20]_1$. The broken rectangles in figures 12*a*, *b* indicate a suitable choice of unit, which we call B, and the unit representation of this boundary is therefore |B.B|. The dot signifies that equivalent atoms in the half periods are relatively displaced by $\frac{1}{2}[001]$ along the tilt axis. To accommodate the minimum misorientation from the ideal lattice each B unit may be associated formally with a $\frac{1}{2}[110]$ lattice dislocation. Figures 13*a*, *b* show the relaxed structure and hydrostatic stress field map of the $\Sigma = 41\,(540)_1$ boundary. This

boundary is centred and each half period of the boundary contains three A units and one B unit, shown by dashed lines. The decomposition of each half period vector is as follows:

$$\tfrac{1}{2}[\bar{4}50]_1 = \tfrac{3}{2}[\bar{1}10]_1 + \tfrac{1}{2}[\bar{1}20]_1.$$

Full lines in figure 13*a* outline $(220)_1$ and $(220)_2$ planes that enter the boundary at a B unit and terminate parallel to the boundary at the next B unit. This suggests that each B unit is located

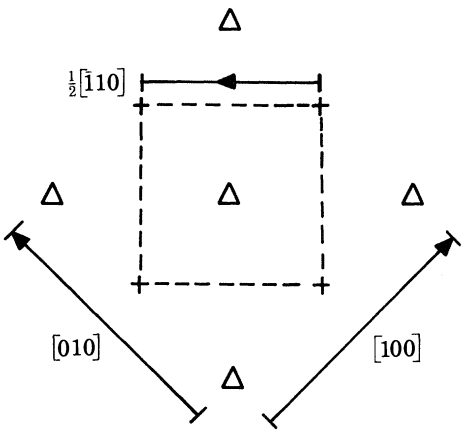

FIGURE 11. [001] Projection of ideal f.c.c. crystal with an A unit shown by broken lines.

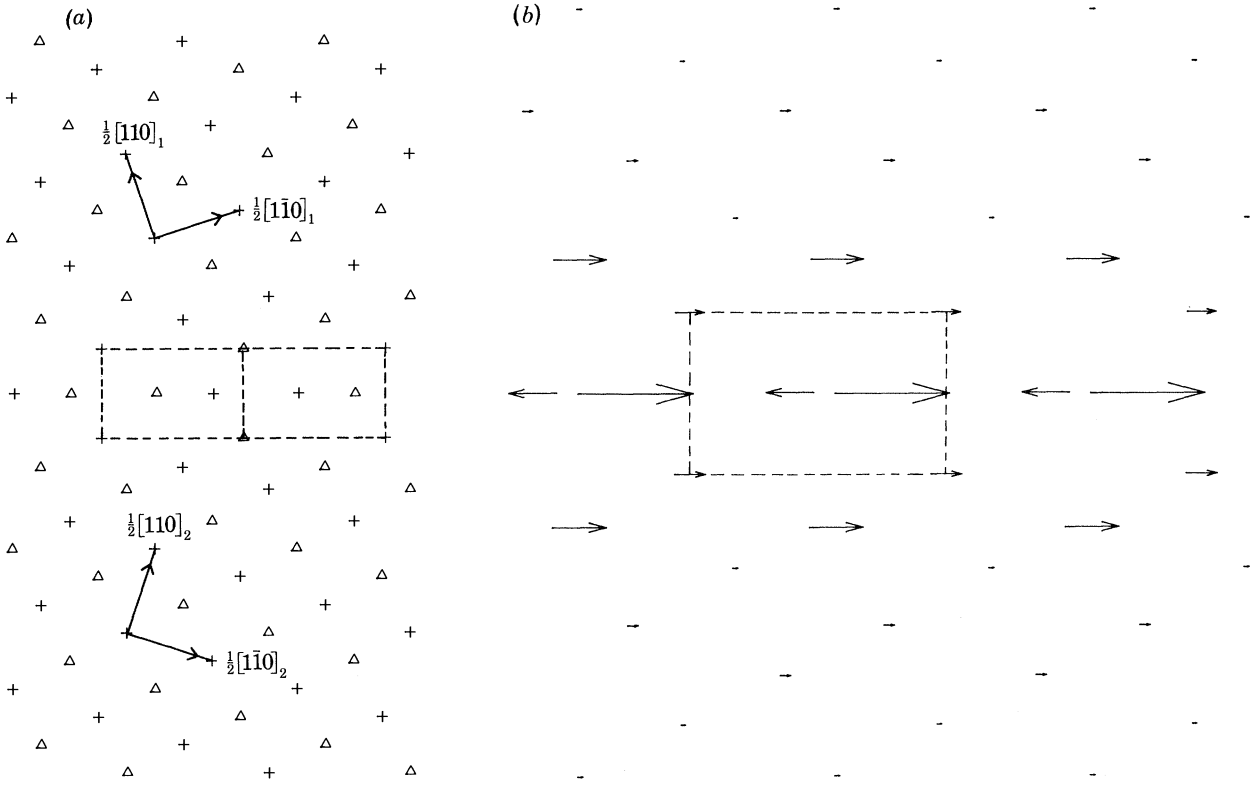

FIGURE 12. (*a*) Relaxed structure of $\Sigma = 5\ (210)_1$, 36.87°/[1$\bar{1}$0] boundary in copper. Two B units, composing one period of the boundary, are shown by broken lines. (*b*) Corresponding hydrostatic stress field map.

at the core of a $\frac{1}{2}[110]$ lattice dislocation, which is consistent with Frank's formula and figure 13*b* where each B unit, shown by broken lines, coincides with the transition from maximum compression to relative tension in the boundary.

As indicated in table 3 the $\Sigma = 37\,(750)_1$ and $\Sigma = 17\,(530)_1$ boundaries are also composed of A and B units and hence it is reasonable to assume that all boundaries in the range $0 < \theta < 36.87°$ are composed of A and B units. It follows that the $\Sigma = 5\,(210)_1$ boundary is favoured. With use

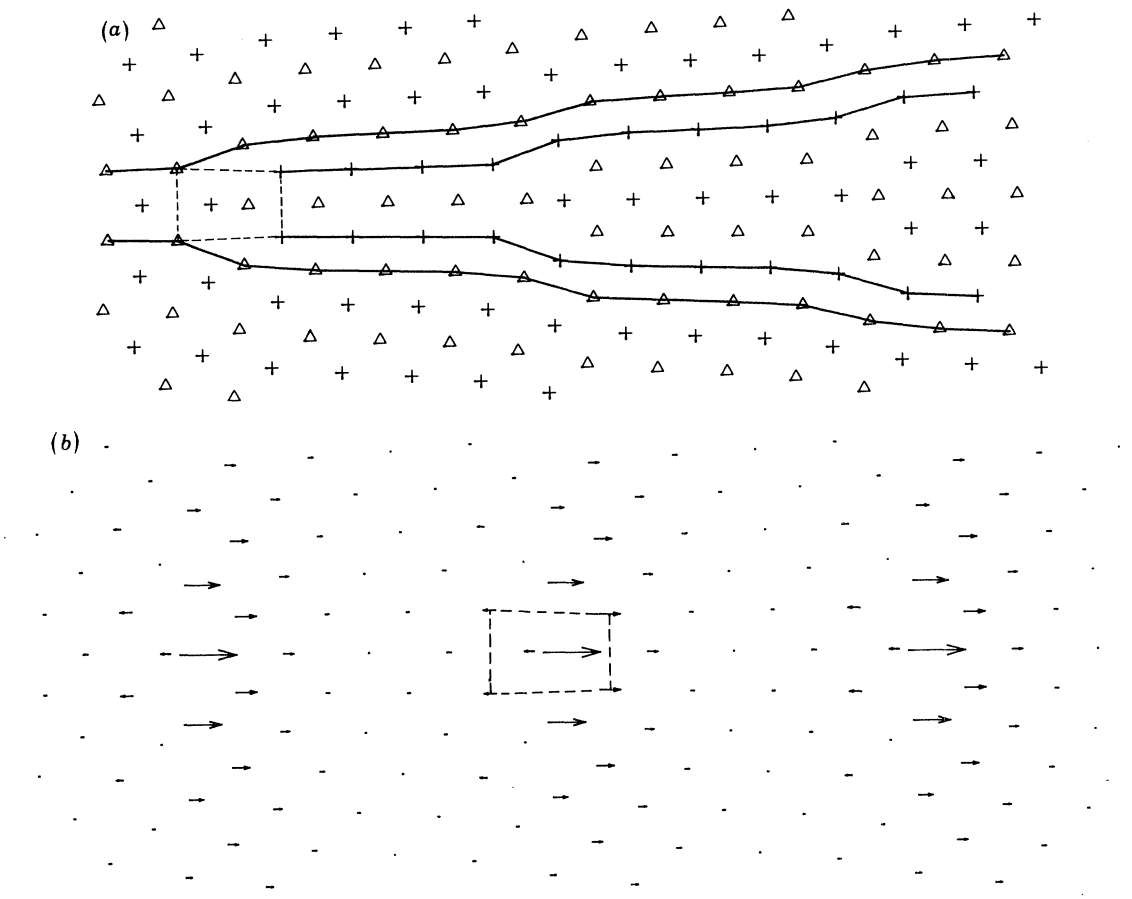

FIGURE 13. (*a*) Relaxed structure of $\Sigma = 41\,(540)_1$, 12.68°/[001] boundary in copper. Broken lines indicate a B unit located at the terminations of $(220)_1$ and $(220)_2$ planes, shown by full lines. (*b*) Corresponding hydrostatic stress field map.

of the principle of continuity of boundary structure the unit representation of any boundary in this range may be found. The 1:1 boundary is $\Sigma = 13\,(320)_1$ for which $\theta = 22.62°$. Hence boundaries in the range $0 \leqslant \theta < 22.62°$ are composed of more A than B units and therefore the most appropriate reference structure is the (110) plane of the ideal crystal with the cores of $\frac{1}{2}[110]$ lattice dislocations located at B units. Boundaries in the range $22.62 < \theta \leqslant 36.87°$ contain more B than A units and it is then most appropriate to regard each A unit as the core of a $-\frac{1}{5}[210]_1$ d.s.c. dislocation preserving the $\Sigma = 5\,(210)_1$ reference structure. Thus the scheme of favoured and non-favoured boundaries, enunciated in §4 for $[1\bar{1}0]$ symmetrical tilt boundaries in aluminium, is equally applicable to these [001] symmetrical tilt boundaries in copper.

6. [11$\bar{1}$] Symmetrical tilt boundaries in aluminium

In the above studies of [1$\bar{1}$0] and [001] symmetrical tilt boundaries it was found that the boundary structure changed continuously with misorientation between two adjacent favoured boundaries. In this section a discontinuous change in boundary structure between two favoured boundaries is found. Near the discontinuity each boundary has two possible structures, differing in their translation states parallel and perpendicular to the tilt axis. Such multiplicity of boundary structures has been reported frequently in the literature (see for example Vitek *et al.* 1980*a*). Below, we suggest that the alternative structures of a boundary may be related to those of other boundaries, nearby in the misorientation range, in the sense that they are composed of the same fundamental structural elements. It is also shown that if a discontinuity in boundary structure does occur between two adjacent favoured boundaries then it is possible that units of mechanically unstable boundaries may exist in the intervening non-favoured boundaries.

In f.c.c. crystals ⟨111⟩ are three-fold inversion axes ($\bar{3}$) and thus the structures of boundaries with misorientations θ and $120-\theta$ are equivalent. Therefore it is sufficient to consider misorientations in the range $0 \leqslant \theta \leqslant 60°$. The boundary plane, misorientation and corresponding Σ value for each boundary selected in this study are given in the first three columns of table 4. The fourth column shows the rigid body translation along the tilt axis, T_z, of the lower grain with respect to the upper grain in units of the lattice parameter, a. The translation T_z is measured with respect to the state where (11$\bar{1}$) planes are continuous across the boundary and hence $-\frac{1}{2\sqrt{3}} \leqslant T_z \leqslant +\frac{1}{2\sqrt{3}}$. The fifth column of table 4 lists the compact polyhedra that are present in the relaxed structures: octahedra, tetrahedra and interlocked trigonal prisms. The period vector, in the upper and lower grain coordinate systems, of each boundary is shown in the sixth column, and the seventh column gives the unit representation of each boundary structure. The structure of $\Sigma = 3\,(1\bar{2}\bar{1})$ was calculated by Pond & Vitek (1977) who regarded it as a symmetrical [101] tilt boundary. Their α and β structures correspond to the structures represented by $|F|$ and $|G|$ respectively. The α structure was observed experimentally by Pond & Vitek (1977).

Centred [11$\bar{1}$] tilt boundaries have centering sites at $\frac{1}{3}$[11$\bar{1}$] and $\frac{2}{3}$[11$\bar{1}$] along the tilt axis. Thus, if a centred [11$\bar{1}$] tilt boundary is favoured, with unit S, its structure is represented by |S.S.S|. Each dot now signifies that equivalent atoms in adjacent S units are relatively displaced by $\frac{1}{3}$[11$\bar{1}$] along the tilt axis. The angle of misorientation is measured with respect to the (1$\bar{1}$0) plane of the ideal crystal, i.e. as $\theta \to 0$ the boundary plane tends to (1$\bar{1}$0) and the period vector tends to the [112] direction. When viewed in projection along [11$\bar{1}$] the (1$\bar{1}$0) plane of the ideal crystal is centred, as shown in figure 14. The appropriate primitive cell of this 'boundary' is therefore bounded by [11$\bar{1}$] and $\frac{1}{6}$[112]. The broken lines in figure 14 outline a suitable unit of this boundary, which we call A. This unit is characterized by $\frac{1}{6}$[112].

Reference to table 4 indicates that there are two groups of boundary structures, defined in overlapping misorientation ranges. The first group is characterized by $T_z \approx 0$ and the fundamental elements appearing in those boundaries are A and B* units. Boundaries in the second group are characterized by $0.235 \leqslant T_z \leqslant 0.283$ and are composed of C, D, E and F units. Furthermore, boundaries in the first group contain octahedra and tetrahedra, whereas in the second group they contain interlocked trigonal prisms. The $\Sigma = 3\,(1\bar{2}\bar{1})_1\,|G|$ structure is exceptional since it belongs to neither group. No boundaries of the second group were found to be mechanically stable in the range $0 \leqslant \theta \leqslant 17.90°$ and also no boundaries of the first group were found to be stable for $38.21 \leqslant \theta \leqslant 60°$. But mechanically stable structures belonging to both groups

PHILOSOPHICAL TRANSACTIONS OF THE ROYAL SOCIETY A MATHEMATICAL, PHYSICAL & ENGINEERING SCIENCES

TABLE 4

boundary plane	θ/deg	Σ	$T_z(a)$	compact polyhedra	period vector	structure
$(7\bar{8}\bar{1})_1/(8\bar{7}1)_2$	13.17	57	−0.017	o., t.	$\frac{1}{2}[325]_1/\frac{1}{2}[235]_2$	|AAAAAB*|
$(6\bar{7}\bar{1})_1/(7\bar{6}1)_2$	15.18	43	−0.014	o., t.	$\frac{1}{2}[8, 5, 13]_1/\frac{1}{2}[5, 8, 13]_2$	|AAAAB*.AAAAB*.AAAAB*|
$(5\bar{6}\bar{1})_1/(6\bar{5}1)_2$	17.90	31	−0.015	o., t.	$\frac{1}{2}[7, 4, 11]_1/\frac{1}{2}[4, 7, 11]_2$	|AAAB*.AAAB*.AAAB*|
$(4\bar{5}\bar{1})_1/(5\bar{4}1)_2$	21.79	21	−0.021	o., t.	$\frac{1}{2}[213]_1/\frac{1}{2}[123]_2$	|AAB*|
$(4\bar{5}\bar{1})_1/(5\bar{4}1)_2$	21.79	21	+0.264	i.t.p.	$\frac{1}{2}[213]_1/\frac{1}{2}[123]_2$	|C|
$(3\bar{4}\bar{1})_1/(4\bar{3}1)_2$	27.80	13	−0.02	o., t.	$\frac{1}{2}[527]_1/\frac{1}{2}[257]_2$	|AB*.AB*.AB*|
$(3\bar{4}\bar{1})_1/(4\bar{3}1)_2$	27.80	13	+0.274	i.t.p.	$\frac{1}{2}[527]_1/\frac{1}{2}[257]_2$	|D.D.D|
$(2\bar{3}\bar{1})_1/(3\bar{2}1)_2$	38.21	7	+0.283	i.t.p.	$\frac{1}{2}[415]_1/\frac{1}{2}[145]_2$	|E.E.E|
$(3\bar{5}\bar{2})_1/(5\bar{3}2)_2$	46.83	19	+0.277	i.t.p.	$\frac{1}{2}[718]_1/\frac{1}{2}[178]_2$	|EF.EF.EF|
$(4\bar{7}\bar{3})_1/(7\bar{4}3)_2$	50.57	37	+0.277	i.t.p.	$\frac{1}{2}[10, 1, 11]_1/\frac{1}{2}[1, 10, 11]_2$	|EFF.EFF.EFF|
$(1\bar{2}\bar{1})_1/(2\bar{1}1)_2$	60	3	+0.235	i.t.p.	$\frac{1}{2}[101]_1/\frac{1}{2}[011]_2$	|F|
$(1\bar{2}\bar{1})_1/(2\bar{1}1)_2$	60	3	−0.028	t.	$\frac{1}{2}[101]_1/\frac{1}{2}[011]_2$	|G|

Abbreviations: i.t.p., interlocked trigonal prisms; o., octahedra; t., tetrahedra.

were found in the range $17.90 < \theta < 38.21°$. The boundaries $\Sigma = 21\,(4\bar{5}\bar{1})_1$ and $\Sigma = 13\,(3\bar{4}\bar{1})_1$ have misorientations in the latter range and two stable structures, one for each group, were found for them. It will be shown below that the energy, γ_2, of boundaries belonging to the second group is a continuous function of misorientation. Since boundaries of the first group are all composed of the same units the energy, γ_1, of these boundaries is also a continuous function of misorientation. The discontinuous change in boundary structure occurs when $\gamma_1(\theta) = \gamma_2(\theta)$

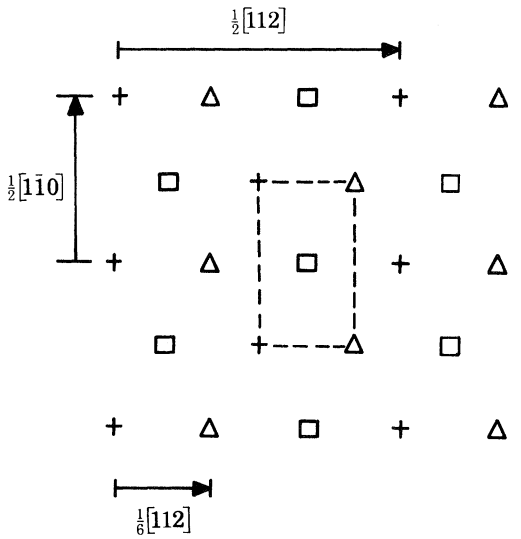

FIGURE 14. $[11\bar{1}]$ Projection of ideal f.c.c. crystal. Broken lines outline an A unit.

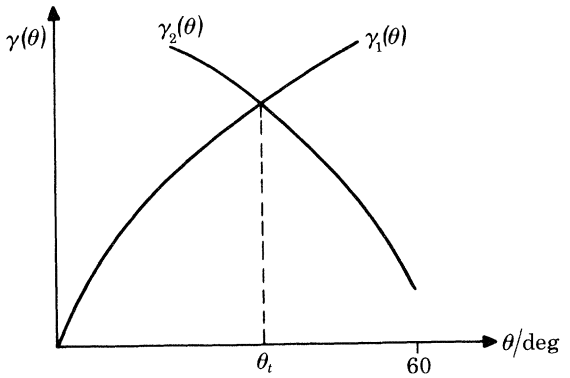

FIGURE 15. Schematic illustration of the energy against misorientation relations for the two groups of boundary structures. A discontinuous change in boundary structure occurs at θ_t.

and this occurs at $\theta = \theta_t$ where $17.90 < \theta_t < 38.21°$. This is illustrated schematically in figure 15. Although the energies of the boundaries cannot be calculated reliably with the cut-off radius used, the ranges in which the two groups of boundaries are stable or unstable concur with the schematic forms of these curves. We shall now present some of the calculated boundary structures to illustrate and substantiate the above points, and then discuss the implications of these results.

Figures 16*a*, *b* show the relaxed structure and hydrostatic stress field of $\Sigma = 21\,(4\bar{5}\bar{1})_1$ belonging to the first group. The coordinate system used throughout this study of $[11\bar{1}]$ symmetrical tilt boundaries is displayed in figure 16*a*. In each period of the boundary there are two A units,

shown by full lines, and one B* unit, shown by broken lines. A pair of $(2\bar{2}0)_1$ and $(2\bar{2}0)_2$ planes is shown (figure 16*a*) entering and terminating parallel to the boundary at a B* unit. This suggests that each B* unit is located at the core of a $\frac{1}{2}[1\bar{1}0]$ lattice dislocation, which is consistent with the hydrostatic stress field map, figure 16*b*. Octahedra and tetrahedra may be seen in the regions of strained crystal between the dislocation cores. The period vector of this boundary is $\frac{1}{2}[213]_1$ and the vector characterizing a B* unit may be deduced as follows:

$$\tfrac{1}{2}[213]_1 - \tfrac{2}{6}[112]_1 = \tfrac{1}{6}[415]_1,$$

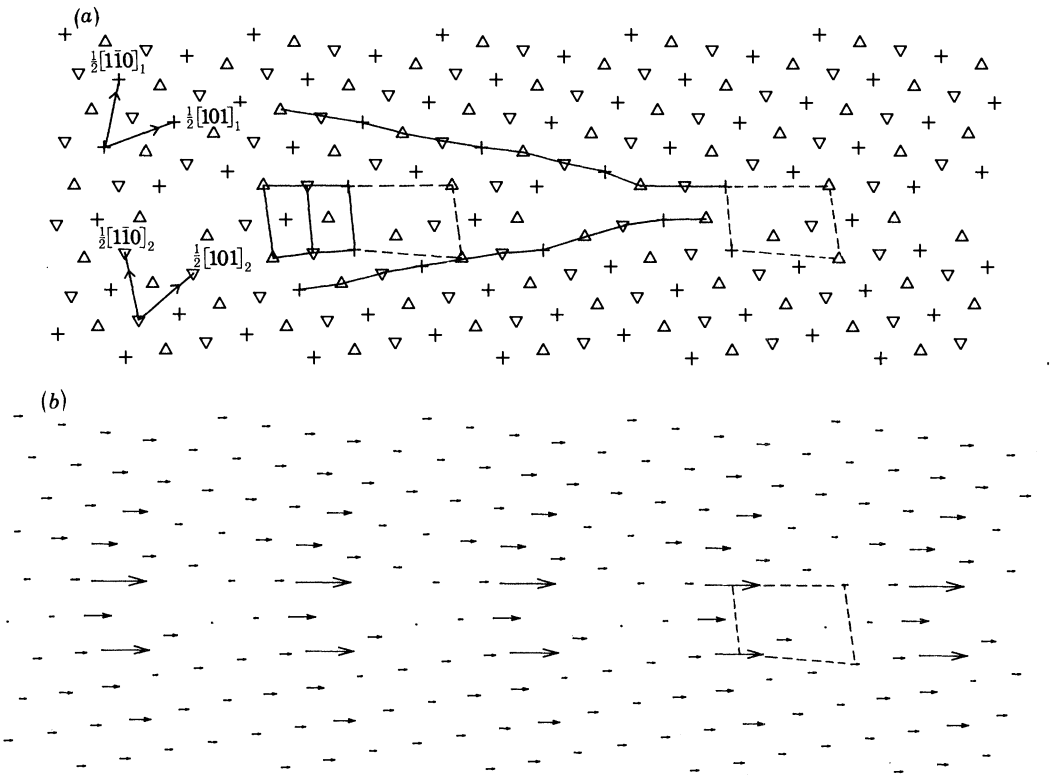

FIGURE 16. (*a*) Relaxed structure of $\Sigma = 21\ (4\bar{5}\bar{1})_1$, 21.79°/$[11\bar{1}]$ boundary in aluminium, belonging to the first group. Two A units and one B* unit, composing one period of the boundary, are shown by full and broken lines respectively. A pair of $(2\bar{2}0)_1$ and $(2\bar{2}0)_2$ planes is shown entering and terminating in the boundary at B* units. (*b*) Corresponding hydrostatic stress field map.

where $\frac{2}{6}[112]_1$ characterizes two A units in each period. $\frac{1}{6}[415]_1$ characterizes a unit of $\Sigma = 7$ $(2\bar{3}\bar{1})_1$ (which is a centred boundary). Following the scheme developed for $[1\bar{1}0]$ and [001] symmetrical tilt boundaries, one would infer that $\Sigma = 7\ (2\bar{3}\bar{1})_1$ is favoured and composed of a contiguous sequence of B* units. However, no such structure of this boundary is mechanically stable and this is the reason for the use of the asterisk. Therefore B* units are not units of the next favoured boundary. The occurrence of B* units in the first group of boundaries must, therefore, be stabilized by A units belonging to the ideal crystal. In other words, the tendency to form regions of relatively undistorted ideal crystal (i.e. A units) is sufficiently strong that the concomitant B* units are stabilized. However, it is anticipated that as the ratio of the number of A units to the number of B* units decreases the boundary structures become less stable. This would indicate that the energy of these boundaries increases with θ, as shown by $\gamma_1(\theta)$ in figure 15.

PHILOSOPHICAL TRANSACTIONS OF THE ROYAL SOCIETY A MATHEMATICAL, PHYSICAL & ENGINEERING SCIENCES

The alternative, mechanically stable structure of $\Sigma = 21\,(4\bar{5}\bar{1})_1$ belongs to the second group of boundaries, and the relaxed structure and hydrostatic stress field map of this boundary are shown in figures 17*a*, *b*. Interlocked trigonal prisms are indicated by overlapping triangles in figure 17*a*. Each $[11\bar{1}]$ period of an i.t.p. consists of two close-packed triangular clusters, which are shown as overlapping triangles. The triangular clusters are separated by approximately $\frac{1}{2}[11\bar{1}]$. The normals of the triangular clusters are mutually inclined and they are also inclined to the $[11\bar{1}]$ axis. The perfection of the clusters increases as θ approaches 60°, where the maximum distortion of the first nearest neighbour separation is *ca.* 1.5 %. This suggests that the energies of

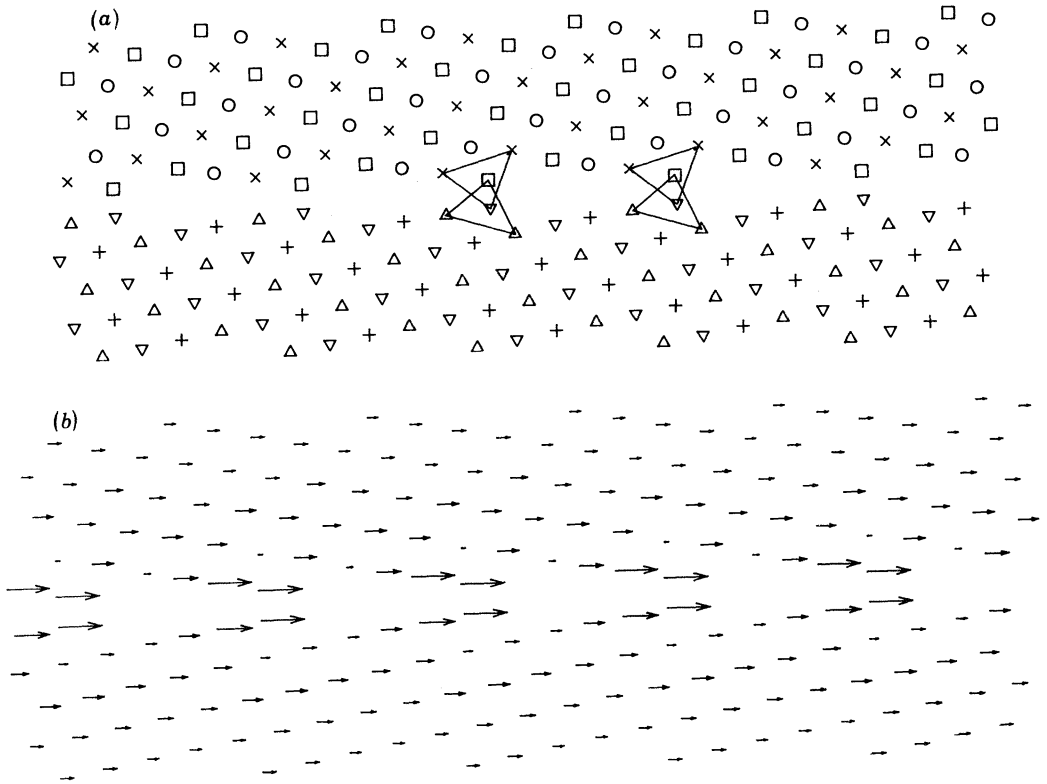

FIGURE 17. (*a*) Relaxed structure of $\Sigma = 21\,(4\bar{5}\bar{1})_1$, 21.79°/$[11\bar{1}]$ boundary in aluminium, belonging to the second group. Overlapping triangles indicate interlocked trigonal prisms. (*b*) Corresponding hydrostatic stress field map.

these boundaries decrease as θ increases, as shown by $\gamma_2(\theta)$ in figure 15. A unit of this boundary is called C and it is characterized by $\frac{1}{2}[213]_1$. A suitable unit is the 'kite-'shaped configuration filling each period of the boundary, similar to a Bishop & Chalmers (1968) structural unit. A pair of $(2\bar{2}0)$ planes terminates at each C unit and thus each C unit may be regarded as the core of a $\frac{1}{2}[1\bar{1}0]$ lattice dislocation. This is consistent with figure 17*b* where $(2\bar{2}0)$ plane terminations coincide with the transition from maximum compression to relative tension in each period. We believe this boundary structure is favoured, although we have not made explicit calculations to confirm that boundaries nearby in the misorientation range contain C units. The reason for this belief will be explained below.

Similar periodic kite configurations were found in the $\Sigma = 13$, 7 and 3 boundary structures, belonging to the second group. Figures 18 and 19 show the relaxed structures of $\Sigma = 7\,(2\bar{3}\bar{1})_1$

and $\Sigma = 3\,(1\bar{2}\bar{1})_1$. The boundary $\Sigma = 7\,(2\bar{3}\bar{1})_1$ is centred and hence each kite (shown by broken lines) occupies one third of a period of the boundary. The overlapping triangles again outline i.t.ps. In figure 19 it is seen that $\Sigma = 3\,(1\bar{2}\bar{1})_1$ consists of a contiguous sequence of interlocked trigonal prisms.

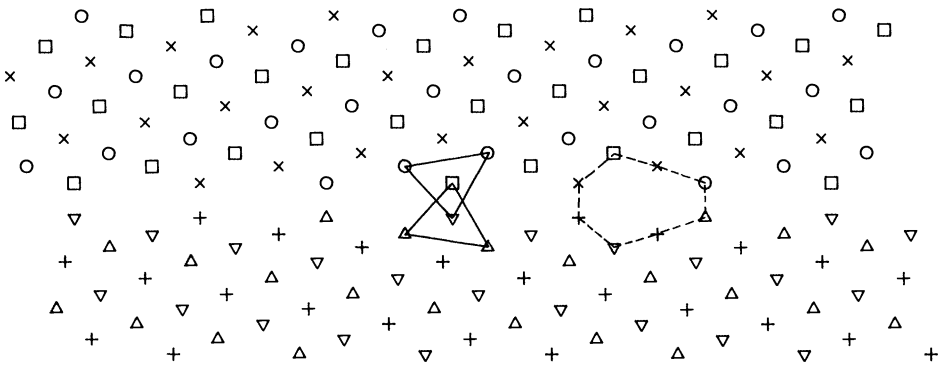

FIGURE 18. Relaxed structure of $\Sigma = 7\,(2\bar{3}\bar{1})_1$, 38.21°/[11$\bar{1}$] boundary in aluminium. An E unit is shown on the right.

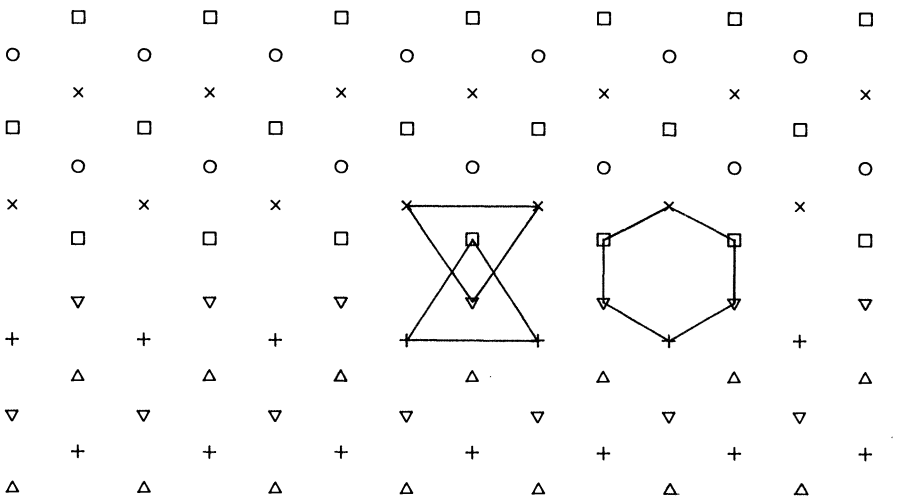

FIGURE 19. Relaxed structure of $\Sigma = 3\,(1\bar{2}\bar{1})_1$, 60°/[11$\bar{1}$] boundary in aluminium. An F unit is shown on the right.

The $\Sigma = 19\,(3\bar{5}\bar{2})_1$ and $\Sigma_1 = (4\bar{7}\bar{3})_1$ relaxed structures are composed of readily identifiable units from $\Sigma = 7\,(2\bar{3}\bar{1})_1$ and $\Sigma = 3\,(1\bar{2}\bar{1})_1$. The latter two boundaries are therefore favoured and we call their units E and F respectively. As an example, figures 20*a*, *b* show the relaxed structure and hydrostatic stress field map of $\Sigma = 37\,(4\bar{7}\bar{3})_1$. This boundary is centred and each third of a period is composed of two F units, shown by full lines, and one E unit, shown by broken lines. Thus the decomposition of each third of a period vector of this $\Sigma = 37$ boundary is as follows:

$$\tfrac{1}{6}[10, 1, 11]_1 = \tfrac{1}{6}[415]_1 + \tfrac{2}{2}[101]_1.$$

In figure 20*b*, F units are located at the transition from maximum compression to relative tension in each third of a period of the boundary. An outlined pair of $(2\bar{4}\bar{2})_1$ and $(4\bar{2}2)_2$ planes is seen

entering the boundary at an F unit and terminating at the next F unit and hence, in the most appropriate g.b.d. description, F units correspond to the cores of $-\frac{1}{6}[1\bar{2}\bar{1}]_1$ d.s.c. dislocations of the $\Sigma = 3$ coincidence system preserving the $(1\bar{2}\bar{1})_1$ boundary.

The structures of $\Sigma = 21\,(4\bar{5}\bar{1})_1$ and $\Sigma = 13\,(3\bar{4}\bar{1})_1$ boundaries belonging to the second group are closely analogous to those of $\Sigma = 7\,(2\bar{3}\bar{1})_1$ and $\Sigma = 3\,(1\bar{2}\bar{1})_1$ since all four boundary structures consist of periodic arrays of contiguous 'kites' and they have very similar translation states. The main difference between these four boundary structures is simply the length of the kites composing

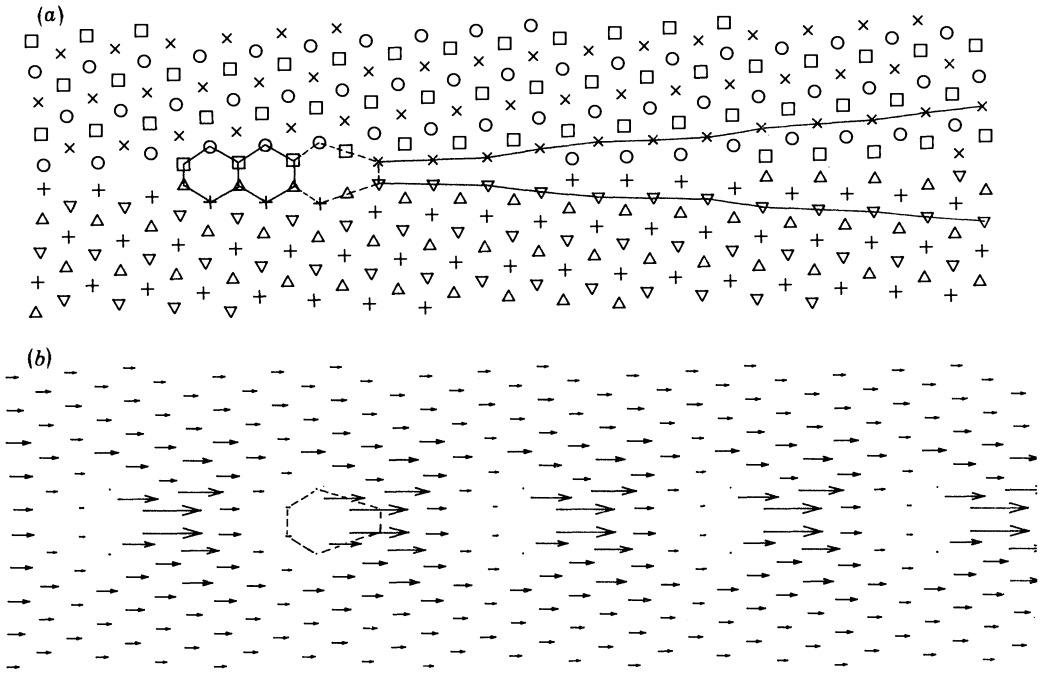

FIGURE 20. (*a*) Relaxed structure of $\Sigma = 37\,(4\bar{7}\bar{3})_1$, 50.57°/[11$\bar{1}$] boundary in aluminium. Two F units and one E unit, composing one third of a period of the boundary, are shown by full and broken lines respectively. $(2\bar{4}\bar{2})_1$ and $(4\bar{2}2)_2$ planes are shown entering and terminating in the boundary at F units. (*b*) Corresponding hydrostatic stress field map.

each boundary. Therefore, in a precisely analogous manner to the mixing of E and F units to produce the structures of all boundaries in the range $38.21 < \theta < 60°$, D and E units can be mixed to produce the structures of all boundaries in the range $27.80 < \theta < 38.21°$. In that case the $\Sigma = 21\,(4\bar{5}\bar{1})_1$ and $\Sigma = 13\,(3\bar{4}\bar{1})_1$ structures of the second group are favoured. Furthermore, it also implies that the energy of all boundaries of the second group, $\gamma_2(\theta)$, is a continuous function of θ and independent of $\gamma_1(\theta)$ since there are no units common to both groups.

The boundary structure changes continuously throughout the misorientation range between two adjacent favoured boundaries only if all the intervening non-favoured boundaries are composed of units from those favoured boundaries. In the present study, the first two adjacent favoured boundaries are '$\Sigma = 1\,(1\bar{1}0)_1$' of the ideal crystal and one of the favoured boundaries of the second group, i.e. $\Sigma = 21\,(4\bar{5}\bar{1})_1$ or $\Sigma = 13\,(3\bar{4}\bar{1})_1$ or $\Sigma = 7\,(2\bar{3}\bar{1})_1$. But these adjacent favoured boundaries have highly incompatible translation states and therefore their units cannot co-exist in intervening non-favoured boundaries. Instead, two independent groups of boundaries are formed in which non-favoured boundaries are composed of units that have

compatible translation states, but no unit is common to both groups. At some misorientation $\theta = \theta_t$ the group of boundaries possessing the lowest energy changes, and then a discontinuous change in boundary structure with misorientation occurs. However the structure of all boundaries at $\theta \neq \theta_t$ is uniquely prescribed; it is only at $\theta = \theta_t$ that two energetically degenerate, non-equivalent, possible structures exist. Thus, provided the units, composing the boundaries on either side of the discontinuity, are known the unit representation of any boundary at $\theta \neq \theta_t$ can be deduced in the manner shown in §4.3. We may speculate that similar discontinuities will arise between other adjacent favoured boundaries whose translation states are incompatible. It is noted that when such a discontinuity occurs a total of four boundary units appear in non-favoured boundaries between the two adjacent favoured boundaries. Only two of those four units belong to necessarily mechanically stable favoured boundary structures. A contiguous sequence of either of the other two units may produce a boundary structure that is not mechanically stable, as for the above B* units. Such units may be said to belong to a pseudo-favoured boundary because they are one of the fundamental structural elements in non-favoured boundaries just like normal favoured boundary units, but the pseudo-favoured boundary is unstable. Discontinuous changes in boundary structure are further discussed in part III.

7. Discussion

A principal result of this paper is that certain boundary units are the fundamental structural elements of other boundaries. These fundamental structural elements cannot be broken down into units of any other boundaries. A boundary that is mechanically stable and composed of a contiguous sequence of only one type of fundamental structural element is favoured. All other boundaries are non-favoured. Since the fundamental structural elements of a favoured boundary are all the same there are no incompatibilities arising from local misorientation differences between adjacent units. A favoured boundary is therefore the most appropriate reference structure for defining the secondary dislocation content of non-favoured boundaries, in which most of the fundamental structural elements are units of that favoured boundary. Every unit of a favoured boundary may also be regarded as the core of a lattice dislocation. Because no two favoured boundary units are the same the lattice dislocation core structure is different in two favoured boundaries, even though the Burgers vectors may be the same; for example, [001] lattice dislocation cores in the favoured $\Sigma = 27\,(115)_1$ and $\Sigma = 11\,(113)_1\,[1\bar{1}0]$ symmetrical tilt boundaries are A and B units respectively. However, because the lattice dislocations composing a high angle boundary are so closely spaced it may be prefereable to describe a favoured symmetrical tilt boundary as the invariant plane of a simple shear and therefore dislocation free.

Non-favoured boundaries are composed of specific arrangements of two different boundary units. Continuity of boundary structure holds throughout the misorientation range between two adjacent favoured boundaries, provided all the intervening boundaries are composed of units from only those two favoured boundaries. The unit representation of any boundary in this range may then be deduced unambiguously, as shown in §4.3. The unit representation supplies, at least qualitatively, the atomic structure and the stress field of the boundary. Fields that are characteristic of edge dislocations exist in all the stress field maps of the relaxed non-favoured boundary structures. The source of these fields may be regarded as the incompatibility normal to the boundary between adjacent units of different types, caused by the local misorientation difference across them. It is remarkable that the boundary units composing non-favoured

boundaries tend to relax to their respective ideal misorientations, even though they may differ from the average misorientation by 20–30°. Local variations in the boundary misorientation are brought about by local bending of planes parallel to the favoured boundaries. This local plane bending is, in turn, effected by coalescence of planes parallel to the macroscopic boundary plane.† For example, consider $\Sigma = 89\,(229)_1$, $34.89°/[110]$ in aluminium, shown in figure 4*a*. Four $(4, 4, 18)_1$ planes and four $(\bar{4}, \bar{4}, 18)_2$ planes, in the upper and lower grains respectively, have coalesced in each period of the boundary. The result of this coalescence of planes, and the relative translation of the two grains, is the formation of three A units and one B unit in each boundary period. However, plane coalescence at a boundary does not imply that the boundary is necessarily non-favoured. For example, $\Sigma = 5\,(210)_1$, $36.87°/[001]$ in copper is favoured but two $(420)_1$ planes have coalesced in each boundary period. The most satisfactory method to demonstrate that a boundary is favoured is to examine the atomic structure and stress fields of neighbouring boundaries in the misorientation range. If the boundary is favoured then different boundary units are introduced at higher and lower angles of misorientation, which do not exist in the favoured boundary structure. Otherwise, the boundary is non-favoured.

The Burgers vectors of secondary intrinsic dislocation, based on favoured boundary reference structures, were not usually primitive d.s.c. vectors. On the other hand, in all cases the Burgers vector was the smallest d.s.c. vector, perpendicular to the corresponding favoured boundary plane, that did not require a step associated with the dislocation core. The absence of steps in the boundary is vital to the description of non-favoured boundaries in terms of favoured boundary units. This point is also discussed in part II where a general formula is presented for the Burgers vector of intrinsic dislocations preserving a favoured tilt boundary.

In tilt boundaries the core structures of positive and negative secondary intrinsic dislocations with Burgers vectors of the same magnitudes, based on favoured boundary reference structures, are not, in general, identical because they contain different boundary units. For example, in §4 it was shown that $\Sigma = 11\,(113)_1$ units are located at the cores of $+\frac{2}{27}[115]_1$ d.s.c. dislocations, preserving $\Sigma = 27\,(115)_1$, whereas $\Sigma = 1\,(001)$ ideal crystal units are located at the cores of $-\frac{2}{27}[115]_1$ dislocations. The implications of this distinction for grain boundary properties are discussed in part III.

Discontinuous changes in boundary structure always occur at favoured boundary orientations, because the units that are introduced into boundaries at $\pm\Delta\theta$ are different. In §6 it was shown that discontinuous changes in boundary structure (henceforth referred to as discontinuities) can also occur between two favoured boundaries. These discontinuities may be expected when the translation states of two adjacent favoured boundaries are incompatible in the sense that their units cannot co-exist in a boundary in equilibrium. There are then two independent series of boundary structures: one series emanating from each favoured boundary. Within each series the boundary structure changes continuously with misorientation. Thus the unit representation of any boundary in either series may be found, as before, once the two units composing boundaries in the series are known. One of these units belongs to the favoured boundary from which the series emanates. The other unit may belong to a pseudo-favoured boundary, i.e. a boundary that is not mechanically stable, but nevertheless its units are fundamental structural elements of non-favoured boundaries. The discontinuity occurs at the misorientation, θ_t, where the energies of the two series are equal, as shown schematically in figure 15. In the interval $\theta_t \pm \delta\theta$ the minimum energy series changes and thus the equilibrium boundary structure transforms. At

† The occurrence of plane coalescence at grain boundaries has also been discussed by Crocker & Faridi (1980).

misorientations near θ_t both series of boundary structures may still be mechanically stable. In that case a boundary near θ_t has two mechanically stable structures that differ in their translation state and their energy. Thus, at least near a discontinuity, some of the alternative, non-equivalent, mechanically stable structures of boundaries may be related, in that they are members of continuous series of boundary structures.

Owing to the neglect of atomic vibrations in these atomistic calculations the bicrystal temperature is effectively 0 K. The boundary energy is therefore the internal energy of the system relative to the ideal crystal. For the same reason that the internal energies, $\gamma_1(\theta)$ and $\gamma_2(\theta)$, of the two series of boundaries represented in figure 15, are continuous, independent functions of θ, we may assume that the entropies $S_1(\theta)$ and $S_2(\theta)$ of the two series are also continuous, independent functions. Hence the free energies of each group of boundaries are also continuous and independent functions of misorientation. In general, the misorientation, θ_t, at which their free energies are equal will vary with temperature because $S_1(\theta) \neq S_2(\theta)$. In other words, the intersection of the two free energy curves will occur at a given boundary misorientation at a certain temperature, and the structure of that boundary will undergo a transformation at that temperature. The possibility of such boundary structure transformations has been discussed by Hart (1972).

It is now possible to provide answers to some of the questions posed in the introduction, at least in the context of symmetrical tilt boundaries.

1. Favoured boundaries are not always associated with the lowest available values of Σ. For example, $\Sigma = 27\ (115)_1$ and $\Sigma = 11\ (113)_1$ are favoured $[1\bar{1}0]$ symmetrical tilt boundaries in aluminium but $\Sigma = 9\ (114)_1$ is not. The present calculations do not suggest that all boundaries with the same value of Σ (or Γ) are favoured. In part II it is shown that, in general, they are not all favoured. Similarly, the present calculations do not suggest that the same boundaries are favoured in metals with the same crystal structure. By comparing the structures of [001] symmetrical tilt boundaries in copper (§5) with those in aluminium (Smith *et al.* 1977) it is seen that grain boundary structure is dependent on the interatomic potential. Therefore variation in boundaries favoured in different metals with the same crystal structure is expected. On the other hand, it will be shown in part III that the boundaries favoured are not governed solely by considerations of energetics: in certain circumstances the occurrence of centred boundaries imposes 'selection rules' on which favoured boundaries may be adjacent. Cusps in the energy against misorientation curve, $\gamma(\theta)$, always occur at favoured boundaries since this is governed by long-range elastic fields (Read & Shockley 1950). However, the cusp depths may be relatively small and therefore indetectable. A more detailed discussion of $\gamma(\theta)$ and other boundary properties is deferred to part III.

2. Non-favoured boundaries are composed of specific sequences of other boundary units. If the boundary structure changes continuously between two adjacent favoured boundaries, then all the intervening non-favoured boundaries are composed of units from the favoured boundaries. The numbers and sequence of favoured boundary units composing any non-favoured boundary are then unique, and may be determined by the methods given in §4.3. To describe the structure of non-favoured boundaries as 'arbitrary' or 'disordered' is therefore misguided. Consider a discontinuity between two adjacent favoured boundaries. The structures of all intervening non-favoured boundaries, except at the discontinuity, are again unique and may be determined once the constituent boundary units are known. At the discontinuity two non-equivalent structures are energetically degenerate, and then the boundary structure is not unique.

PHILOSOPHICAL TRANSACTIONS OF THE ROYAL SOCIETY A MATHEMATICAL, PHYSICAL & ENGINEERING SCIENCES

The hydrostatic stress field maps show that intrinsic g.b.ds are distinct and localized at all misorientations between two favoured boundaries. This maintains even at 1:1 boundaries where the density of intrinsic dislocations, based on the appropriate favoured boundary reference structures, is highest. The cores of those intrinsic secondary dislocations are always separated by at least one boundary unit: 'core overlap' does not occur.

3. In any non-favoured boundary, g.b.d. stress field sources exist at the intermittences of the sequence of majority elemental units caused by minority elemental units. The minority units may therefore be regarded as the cores of secondary intrinsic g.b.ds preserving the boundary composed of a continuous sequence of the majority units. As the misorientation from a favoured boundary increases, the 'majority' and 'minority' units are interchanged at the 1:1 boundary. At the 1:1 boundary both g.b.d. descriptions are equally appropriate, and the transition from one description to the other takes place. The change in atomic structure with boundary misorientation is accomplished at intrinsic g.b.d. cores, which are units from the next favoured boundary if the boundary structure changes in a continuous manner. When a discontinuity occurs between two adjacent favoured boundaries, units of the 'next' favoured boundary are introduced only at misorientations beyond the discontinuity. The units introduced before the discontinuity belong to another boundary structure, which may or may not be mechanically stable.

4. Any property that depends only on the structure of the boundary core can be used to determine favoured boundaries. Thus the variation of the grain boundary diffusion coefficient with misorientation is suitable, but the grain boundary energy is not. This is because the boundary structure changes discontinuously at favoured boundary orientations, but the long-range field of the boundary behaves similarly at both favoured boundary and short-period non-favoured boundary orientations. A full discussion is again deferred to part III.

In this final section we shall discuss the results of some earlier atomistic studies of symmetrical tilt boundaries in the light of this work. Most previous atomistic studies have treated only short-period boundaries. Hasson *et al.* (1972) calculated the structures of several symmetrical [001] tilt boundaries using a Morse potential constructed for aluminium. Each period of their $\Sigma = 73\,(11, 5, 0)_1$ boundary structure is composed of four units from their $\Sigma = 5\,(210)_1$ boundary and one unit from their $\Sigma = 5\,(310)_1$ boundary. Vitek *et al.* (1980*b*) calculated the structure of several [001] and $[1\bar{1}0]$ symmetrical tilt boundaries using a variety of potentials constructed for b.c.c. metals. One example from this work is the decomposition of each half period of the (centred) $\Sigma = 11\,(113)_1$ boundary into one unit from the (centred) $\Sigma = 9\,(114)_1$ favoured boundary and one unit from the 'reflexion twin' structure of the $\Sigma = 3\,(112)_1$ boundary:

$$\tfrac{1}{2}[33\bar{2}]_1 = \tfrac{1}{2}[22\bar{1}]_1 + \tfrac{1}{2}[11\bar{1}]_1.$$

The broken squares in figure 8 of that paper corresponds to one unit of the reflexion twin shown in figure 8.12*a* of Christian (1975). An interesting case arose in Smith *et al.* (1977) who calculated the structure of several [001] symmetrical tilt boundaries in aluminium using the same potential as in the present work. Our discussion is confined to the $\Sigma = 5\,(210)_1$ and $\Sigma = 5\,(310)_1$ boundaries. which are favoured, and the $\Sigma = 29\,(520)_1$ and $\Sigma = 29\,(730)_1$ boundaries which are non-favoured and lie in the misorientation range between the $\Sigma = 5$ boundaries. Smith *et al.* (1977) show that the $(520)_1$ boundary is composed of a 1:1 mixture of units from the $\Sigma = 5$ boundaries. It is important to note that the translation states of the two $\Sigma = 5$ boundaries are highly compatible. One would therefore expect continuity of boundary structure to occur throughout the

misorientation range between them. In that case the $(730)_1$ boundary should contain two (210) units and one $(310)_1$ unit, as indicated by the decomposition of its period vector:

$$\tfrac{1}{2}[\bar{3}70]_1 = \tfrac{2}{2}[\bar{1}20]_1 + \tfrac{1}{2}[\bar{1}30]_1.$$

Smith *et al.* (1977) correctly point out that their $(730)_1$ boundary structure cannot be described in this way. Indeed the translation state of their $(730)_1$ structure prohibits the existence of units from the $\Sigma = 5$ favoured boundaries. The present authors have recalculated the structure of the $(730)_1$ boundary, using the same potential. In addition to the relaxed structure, given by Smith *et al.*, we found a relaxed stable structure conforming to the above description in terms of $\Sigma = 5$, as expected. The calculated energy of the latter structure is 26% less than that of the structure found by Smith *et al.*, although not very much credence may be attached to the calculated energies. This example illustrates the capacity of the present model to describe the structures of high-angle grain boundaries.

We are very grateful to Professor J. W. Christian, F.R.S., for many helpful comments and enlightenment about the multiplicity of dislocation descriptions of interfaces.

A useful discussion was also held with Dr R. C. Pond of the University of Liverpool. This research was supported by the National Science Foundation, MRL Program, contract no. DMR79–23647.

References

Aust, K. T. & Rutter, J. W. 1959 *Trans. Am. Inst. Min. metall. Engrs* **215**, 820.
Balluffi, R. W. 1980 *Interfacial segregation* (ed. W. C. Johnson & J. M. Blakely), p. 193. Cleveland, Ohio: American Society for Metals.
Basinski, Z. S., Duesbery, M. S. & Taylor, R. 1971 *Can. J. Phys.* **49**, 2160.
Bilby, B. A. 1955 *Rep. Conf. on Defects in Crystalline Solids*, p. 124. London: The Physical Society.
Bishop, G. H. & Chalmers, B. 1968 *Scr. metall.* **2**, 133.
Bishop, G. H. & Chalmers, B. 1971 *Phil. Mag.* **24**, 515.
Bollmann, W. 1970 *Crystal defects and crystalline interfaces*. Berlin: Springer-Verlag.
Brandon, D. G., Ralph, B., Ranganathan, S. & Wald, M. S. 1964 *Acta Metall.* **12**, 813.
Bristowe, P. D. & Crocker, A. G. 1978 *Phil. Mag.* **38**A, 487.
Christian, J. W. 1975 *The theory of transformations in metals and alloys*, part I. Oxford: Pergamon Press.
Christian, J. W. & Crocker, A. G. 1980 *Dislocations in solids* (ed. F. R. N. Nabarro), vol. 3, p. 165. Amsterdam: North-Holland.
Crocker, A. G., Doneghan, M. & Ingle, K. W. 1980 *Phil. Mag.* **41**A, 21.
Crocker, A. G. & Faridi, B. A. 1980 *Acta metall.* **28**, 549.
Dagens, L., Rasolt, M. & Taylor, R. 1975 *Phys. Rev.* B**11**, 2726.
Duesbery, M. S., Vitek, V. & Bowen, D. K. 1973 *Proc. R. Soc. Lond.* A **332**, 85.
Egami, T., Maeda, K. & Vitek, V. 1980 *Phil. Mag.* **41**A, 883.
Frank, F. C. 1950 *Symposium on the Plastic Deformation of Crystalline Solids*, p. 150. London: The Physical Society.
Gleiter, H. 1977*a* *Phil. Mag.* **36**A, 1109.
Gleiter, H. 1977*b* *Scr. metall.* **11**, 305.
Goodhew, P. J. 1980 *Grain boundary structure and kinetics* (ed. R. W. Balluffi), p. 155. Cleveland, Ohio: American Society for Metals.
Hart, E. W. 1972 *The nature and behavior of grain boundaries* (ed. H. Hu), p. 155. New York: Plenum Press.
Hasson, G., Boos, J. Y., Herbeuval, I., Biscondi, M. & Goux, C. 1972 *Surf. Sci.* **31**, 115.
Hirth, J. P. & Balluffi, R. W. 1973 *Acta metall.* **20**, 199.
Ingle, K. W. & Crocker, A. G. 1980 *Phil. Mag.* **41** A, 713.
Jacucci, G. & Taylor, R. 1981 *J. Phys.* F **9**, 787.
Jacucci, G., Taylor, R., Tenenbaum, A. & van Doan, N. 1981 *J. Phys.* F **9**, 793.
King, A. H. & Smith, D. A. 1980 *Acta crystallogr.* A **36**, 335.
Kronberg, M. L. & Wilson, F. H. 1949 *Trans. Am. Inst. Min. metall. Engrs.* **185**, 50.
Pond, R. C. & Smith, D. A. 1977 *Phil. Mag.* **36**A, 353.
Pond, R. C., Smith, D. A. & Vitek, V. 1978 *Scr. metall.* **12**, 669.
Pond, R. C. & Vitek, V. 1977 *Proc. R. Soc. Lond.* A**357**, 453.

PHILOSOPHICAL TRANSACTIONS OF THE ROYAL SOCIETY A MATHEMATICAL, PHYSICAL & ENGINEERING SCIENCES

Pond, R. C., Vitek, V. & Smith, D. A. 1979 *Acta. metall.* **27**, 235.
Pumphrey, P. H. 1976 *Grain boundary structure and properties* (ed. G. A. Chadwick & D. A. Smith), p. 139. London, New York: Academic Press.
Pumphrey, P. H., Gleiter, H. & Goodhew, P. 1977 *Phil. Mag.* **36**A, 1099.
Pumphrey, P. H. & Goodhew, P. J. 1979 *Phil. Mag.* **39**A, 825.
Read, W. T. & Shockley, W. 1950 *Phys. Rev.* **78**, 275.
Smith, D. A., Vitek, V. & Pond, R. C. 1977 *Acta metall.* **25**, 475.
Sutton, A. P. 1981 Ph.D. thesis, University of Pennsylvania.
Sutton, A. P. 1982 *Phil. Mag.* **46**A, 171.
Sutton, A. P., Balluffi, R. W. & Vitek, V. 1981 *Scr. metall.* **15**, 989.
Sutton, A. P. & Vitek, V. 1980*a* *Scr. metall.* **14**, 563.
Sutton, A. P. & Vitek, V. 1980*b* *Scr. metall.* **14**, 129.
Sutton, A. P. & Vitek, V. 1981 *Proc. Int. Conf. Dislocation modelling of Physical Systems* (ed. M. F. Ashby, R. Bullough, C. S. Hartley & J. P. Hirth), p. 549. Oxford: Pergamon Press.
Sutton, A. P. & Vitek, V. 1982 *Acta metall.* **30**, 2011.
Taylor, R. 1981 *Interatomic potentials and crystalline defects* (ed. J. K. Lee), p. 71. New York: The Metallurgical Society of American Institute of Mining, Metallurgical and Petroleum Engineers.
Vitek, V. 1975 *Scr. metall.* **9**, 611.
Vitek, V., Smith, D.A . & Pond, R. C. 1980*b* *Phil. Mag.* **41**A, 649.
Vitek, V., Sutton, A. P., Smith, D. A. & Pond, R. C. 1979 *Phil. Mag.* **39**A, 213.
Vitek, V., Sutton, A. P., Smith, D. A. & Pond, R. C. 1980*a* *Grain boundary structure and kinetics* (ed. R. W. Baluffi), p. 115. Cleveland, Ohio: American Society for Metals.
Vitek, V., & Yamaguchi, M. 1981 *Interatomic potentials and crystalline defects* (ed. J. K. Lee), p. 223. New York: The Metallurgical Society of American Institute of Mining, Metallurgical and Petroleum Engineers.

PHILOSOPHICAL TRANSACTIONS OF THE ROYAL SOCIETY A MATHEMATICAL, PHYSICAL & ENGINEERING SCIENCES